Lagrangian Voronoï meshes and particle dynamics with shocks

Bruno Després*†

July 20, 2023

Abstract

We present a new first order numerical method on lagrangian Voronoï moving meshes for the numerical simulation of compressible flows with shocks and internal interfaces between different gas. The method is based on the closed form formula of the partial derivative of the volume of Voronoï cells with respect to the generators. The mathematical proof of the formula seems original with respect to the literature. A corollary is that the volume of Voronoï cells is generically of class C^1 with respect to the generators. The final scheme is conservative in local mass, total momentum and total energy, and it is endowed with an entropy inequality which insures the correctness of shocks calculations. Numerical illustrations in dimension $d = 2$ are displayed for basic problems on coarse meshes. The implementation developed to obtain the numerical illustrations uses a freely available library for the generation of the Voronoï cells at all time steps.

1 Introduction

We present the mathematical and numerical foundations of a discrete scheme based on lagrangian Voronoï moving meshes adapted to the numerical simulation of compressible flows with shocks and internal interfaces between different gas. This method can be understood as the combination of two different classes of numerical methods.

The first class of methods concerns Voronoï meshes [22] on moving points [2, 19, 15]. In such methods one recalculates the mesh from some special points called generators at every time step. The initial motivation for the present work was mathematical issues raised by the recent remarkable use [32] of quasi-Voronoï mesh techniques for astrophysical flows and compressible fluid flows. In particular, we refer again to [32], the local connectivity of Voronoï meshes can be arbitrary, so Voronoï meshes are attractive to remove some mesh viscosity which may show up with more traditional lagrangian solvers. These works found a recent extension in [18].

The second class of numerical methods is particle methods for compressible flow dynamics with shocks. Many different particle methods exist. The smooth particle hydrodynamics (SPH) [28, 34] was developed initially in the astrophysical community. The particle in cell (PIC) method [8, 4] is concerned with the coupling of charged particles with a Poisson solver or a Maxwell solver. Lagrangian solvers [1, 6, 14, 7, 27, 26] are not traditionally considered as particle methods but more as methods on moving grids. Since the mass of individual cells is constant in these solvers by construction, lagrangian solvers can be considered as specific particles methods as well, even if the frozen connectivity of the mesh induces strong constraints on the cells displacement. Actually the already quoted works [32, 18] use more quasi-Voronoï and they allow mass fluxes across the cell boundaries. In a different language, one would say these method are Arbitrary Lagrange-Euler (ALE) techniques. Also in [25] which is an assembly of different techniques, a two-steps scheme is developed where the first step is based on a purely lagrangian solver and the second step is Voronoï remeshing (so it is ultimately an ALE scheme).

To our knowledge, the mathematical foundations of moving Voronoï mesh techniques interpreted as particle methods are not discussed per se in the literature. Hereafter, we adopt an axiomatic viewpoint. That is we explore if it is possible to develop numerical methods which on the one hand are based on **rigorous** lagrangian Vononoï meshes and which on the other hand can be interpreted as particle methods which **rigorously** preserve mass, total impulse and total energy and for which an additional discrete entropy inequality can be proved. We will show that a positive answer exists to these questions. It will result in the construction of an original first order (space and time) numerical scheme which will be analyzed and illustrated with basic test problems. The implementation of the scheme takes advantage of the fact that Voronoï librairies of excellent quality are freely available. This method can be the basis of more elaborated methods where all the arsenal of modern computational fluid dynamics techniques (high-order techniques, non linear limiters, various remeshing techniques) can be introduced to enhance the final quality of practical simulations. These issues are not discussed hereafter and are left for further research.

*Sorbonne Université, LJLL, despres@ann.jussieu.fr

†The author deeply thanks Stéphane Del Pino, Emmanuel Labourasse and François Hermeline for many fruitful scientific discussions during the elaboration stage of this work.

To formalize the main mathematical and numerical questions addressed in this work we introduce some notations. Let $\Omega \subset \mathbb{R}^d$ ($d \geq 1$) be a regular non empty open bounded domain which is additionally supposed to be a convex polytope for the simplicity of the presentation (in the numerical test Section 5, Ω will be chosen to be a rectangle). Let $\mathbf{x}_i \in \Omega$, $1 \leq i \leq N$, be a finite number of generators (also called centroids). These generators are our particles, even if we will refer to them as the generators. The Voronoï cell generated by $\mathbf{x}_i$ is defined as

$$\Omega_i = \{\mathbf{x} \in \Omega \text{ such that } |\mathbf{x} - \mathbf{x}_i| < |\mathbf{x} - \mathbf{x}_k| \text{ for } k \neq i\} \subset \Omega, \qquad 1 \leq i \leq N. \tag{1}$$

Since we will assume without condition that the generators are different

$$\mathbf{x}_i \neq \mathbf{x}_k, \quad \text{for all } 1 \leq i \neq k \leq N, \tag{2}$$

then the Voronoï cells are non empty $\Omega_i \neq \emptyset$. By construction, the Voronoï cell Ω_i is an open convex polytope [2]. Its d-dimensional measure, referred to as its volume in the rest of this work, is

$$|\Omega_i| = \int_{\mathbf{x} \in \Omega_i} dx > 0 \tag{3}$$

In numerical particle dynamics, a constant-in-time mass is attached to points. Specifically $M_i > 0$ will denote the mass attached to the generator $\mathbf{x}_i$. The mass is the product of the density $\rho_i > 0$ of the particle times the volume of the particle, that is $M_i = \rho_i |\Omega_i|$. Following the classical Lagrange principe, the mass is constant in time during any kind of evolution process. In such evolution process the generators move. They will be denoted as $\mathbf{x}_i(t)$ for a time-continuous evolution, and $\mathbf{x}_i^n$ for a time-discrete scheme where $n \in \mathbb{N}$ is the iteration index, and $t_n = n\Delta$ is the corresponding time. Similarly, the volume will be denoted as $|\Omega_i|(t)$ or $|\Omega_i|^n$. For the simplicity of the exposure, we concentrate on a time-continuous evolution, and time-discrete schemes will be obtained by an immediate explicit Euler technique. In the context of a time-continuous evolution, the time derivative of the specific volume $\tau_i(t) = \rho_i(t)^{-1} > 0$ is given by the chain rule

$$M_i \frac{d}{dt}\tau_i(t) = \frac{d}{dt}|\Omega_i| = \sum_k \left\langle \nabla_{\mathbf{x}_k}|\Omega_i|(t), \frac{d}{dt}\mathbf{x}_k(t) \right\rangle. \tag{4}$$

This formula is the basis of lagrangian flow solvers such as [1, 6, 14, 7, 27, 26]. To be able to use it in in our context, we need to address some issues.

The first difficulty: it concerns the calculation in closed form of the partial derivatives $\nabla_{\mathbf{x}_k}|\Omega_i|$. Due to the very unpredictable nature of how a Voronoï cell Ω_i depends on all generators $\mathbf{x}_k$ in the vicinity of the Voronoï cell, it is even conceivable at first examination that $|\Omega_i|$ might be a discontinuous function of the neighboring generators. The unpredictability comes the reconnection process which is common for Voronï meshes on moving generators. For example, the number of neighboring Voronoï generators to one Voronï cell is clearly a discontinuous function. So the volume $|\Omega_i|$ might be as well a discontinuous function with respect to the generators. Actually it is opposite, in the sense that a closed form formula $\nabla_{\mathbf{x}_k}|\Omega_i|$ can be justified in all dimension $d \geq 1$, and that $|\Omega_i|$ is generically of class C^1 because $\nabla_{\mathbf{x}_k}|\Omega_i|$ is generically a continuous function with respect to the generators.

The second difficulty: one needs to define the velocities $\mathbf{v}_i(t) = \frac{d}{dt}\mathbf{x}_i(t)$ for all $1 \leq i \leq N$ such that basic principles in computational fluid dynamics are satisfied. We will use the system of compressible non viscous Euler equations as a model problem. We will show that it is possible to satisfy some important principles such as mass preservation, total momentum preservation, total energy preservation and increase of the physical entropy. We will explain in the appendix that the gradient operator which is constructed (in particular for the discretization of the gradient of the pressure) is weakly consistant (a notion which comes from Lax).

A third difficulty: many particle methods have stability issues and the new particle scheme is no exception when the dynamics of some generators is such that they become very close. In view of the condition (2), this is a singular behavior. That is why we will develop a stabilization algorithm to enhance the range of use of the method by making sure that the generators cannot coincide.

The organization of this work is as follows. Section 2 solve the main mathematical difficulty for lagrangian Voronoï meshes, which is the calculation the gradient of the Voronoï volumes. The main Theorem of this work yields a characterization of the differential properties of of lagrangian Voronoï cells. In particular an original formula is proposed which explains that the measure (the volume in 3D) of lagrangian Voronoï cells is a C^1 function with respect to the generators (called the centroïds of the Voronoï mesh). In Section 3, the previous results are used to define an original lagrangian fluid solver. The model equations are the entropy consistant compressible Euler equations in general dimension $\mathbf{x} \in \mathbb{R}^d$. The solver is first order at most in space and time. It is conservative in mass, total momentum and total energy, and it comes with a stabilization technique which can be used to avoid degenerate situations. The Section 4 presents two enhancements of the method (still at first order). Some very basic numerical illustrations are proposed in the numerical Section 5. In the appendix, we provide a justification of the weak consistency of our approach.

2 Lagrangian Voronoï meshes

As discussed previously, the first difficulty is to calculate in closed form the partial derivatives $\nabla_{\mathbf{x}_k}|\Omega_i|$. To the best of the author's knowledge, standard tools in computational geometry provide useful algorithms based on the chain rule to calculate the numerical value of partial derivatives [22, 2, 19, 15, 3, 24], but do not provide a closed form formula. In order to calculate $\nabla_{\mathbf{x}_k}|\Omega_i|$ in closed form, we follow recent works in applied statistical physics [17, 30] by introducing partition functions

$$Z_i^\beta(\mathbf{x}:\mathbf{x}_1,\ldots,\mathbf{x}_N)=\frac{e^{-\beta|\mathbf{x}-\mathbf{x}_i|^2}}{\sum_{k=1}^N e^{-\beta|\mathbf{x}-\mathbf{x}_k|^2}},\qquad 1\leq i\leq N,$$

where the positive parameter $\beta>0$ has the scaling of the inverse of a temperature in statistical physics. By construction, one has that $0<Z_i^\beta<1$ and that $\sum_{i=1}^N Z_i^\beta=1$. The interest of the partition function is that one can avoid to study in too much details the local geometry of Voronoï cells. In dimension $d=2$, it is possible to rely on a local geometrical parametrization of Voronoï cells to calculate the partial derivatives as shown in [16], even if the number of local geometrical configurations to examine can be important. However in dimension $d\geq 3$, it seems almost impossible to cover all possible geometrical configurations. For these reasons, the use of partitions functions provides an interesting alternative. However, in these quoted references [17, 30], the partition functions are studied with mostly heuristic arguments (see [30, Appendix E]). In this Section, we justify the results [30] by studying the convergence $\beta\to+\infty$ of the partitions functions in general dimension. The final part of our proof uses the dominated convergence of Lebesgue which allows to obtain the final result in full rigor. A preliminary natural result is the following.

Proposition 2.1. *One has the limit*

$$|\Omega_i|=\lim_{\beta\to+\infty}\int_{\mathbf{x}\in\Omega} Z_i^\beta(\mathbf{x}:\mathbf{x}_1,\ldots,\mathbf{x}_N)dx\quad \textit{for all } i. \tag{5}$$

Our proof is based on an elementary result.

Lemma 2.2. *There exists $C>0$ such that*

$$\int_{\mathbf{x}\in\Omega_j} Z_i^\beta(\mathbf{x}:\mathbf{x}_1,\ldots,\mathbf{x}_N)dx\leq\frac{C}{\beta}\qquad \textit{for all } i\neq j. \tag{6}$$

Proof. One has the natural bounds $0\leq Z_i^\beta(\mathbf{x}:\mathbf{x}_1,\ldots,\mathbf{x}_N)\leq\frac{e^{-\beta|\mathbf{x}-\mathbf{x}_i|^2}}{e^{-\beta|\mathbf{x}-\mathbf{x}_j|^2}}\leq e^{-\beta f_{ij}(\mathbf{x})}$ where we note

$$f_{ij}(\mathbf{x})=|\mathbf{x}-\mathbf{x}_i|^2-|\mathbf{x}-\mathbf{x}_j|^2=2\left\langle\mathbf{x}-\frac{\mathbf{x}_i+\mathbf{x}_j}{2},\mathbf{x}_j-\mathbf{x}_i\right\rangle,\qquad 1\leq i\neq j\leq N. \tag{7}$$

Since Ω_j is the Voronoï cell centered on $\mathbf{x}_j$, one has $0\leq f_{ij}(\mathbf{x})$ for $\mathbf{x}\in\Omega_j$. The function f_{ij} vanishes if and only if $\left\langle\mathbf{x}-\frac{\mathbf{x}_i+\mathbf{x}_j}{2},\mathbf{x}_j-\mathbf{x}_i\right\rangle=0$. This is the equation of an hyperplane which separates two half-spaces as illustrated in Figure 1. One has that $\Omega_i\subset\left\{\left\langle\mathbf{x}-\frac{\mathbf{x}_i+\mathbf{x}_j}{2},\mathbf{x}_j-\mathbf{x}_i\right\rangle<0\right\}$ is in one half-plane while $\Omega_j\subset$

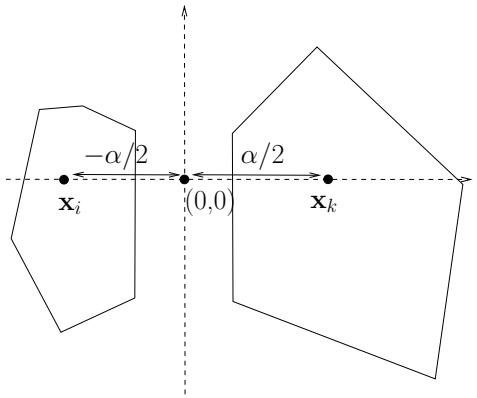

Figure 1: The separating plane in dimension two. The Voronoï cells can touch as well.

$\left\{\left\langle\mathbf{x}-\frac{\mathbf{x}_i+\mathbf{x}_j}{2},\mathbf{x}_j-\mathbf{x}_i\right\rangle>0\right\}$ is in the other half-plane. So the two Voronoï cells are separated by the hyperplane and the mid-point stands on the hyperplane. It is always possible to assume that the frame has been chosen

so that the first axis is aligned with $\mathbf{x}_j - \mathbf{x}_i$. One can start from an arbitrary frame and perform a rotation-translation of the frame so that this alignment condition is fulfilled. In the aligned frame one has $\frac{\mathbf{x}_i+\mathbf{x}_j}{2} = 0$, $\mathbf{x}_i = (-\alpha/2, 0, \dots, 0)$ and $\mathbf{x}_j = (\alpha/2, 0, \dots, 0)$ where $\alpha = |\mathbf{x}_i - \mathbf{x}_j| > 0$. Since the Lebesgue measure is invariant by translation-rotation, all integrals can be evaluated in the aligned frame. One obtains

$$\int_{\mathbf{x}\in\Omega_j} e^{-\beta f_{ij}(\mathbf{x})} dx = \int_{(x_1,\dots,x_d)\in\Omega_j} e^{-\beta x_1} dx_1 \dots dx_d \leq \mathrm{diam}(\Omega)^{d-1} \int_{x_1>\alpha/2>0} e^{-\beta\alpha x_1} dx_1 \leq \frac{1}{\alpha\beta}\mathrm{diam}(\Omega)^{d-1}.$$

Varying the indices $i \neq j$, one obtains the claim with the constant $C = \frac{\mathrm{diam}(\Omega)^{d-1}}{\min_{1\leq i\neq j\leq N}|\mathbf{x}_i-\mathbf{x}_j|}$. □

End of the proof of Proposition 2.1. For a given $1 \leq i \leq N$, one has the decomposition

$$\int_{\mathbf{x}\in\Omega} Z_i^\beta(\mathbf{x} : \mathbf{x}_1, \dots, \mathbf{x}_N) dx = \int_{\mathbf{x}\in\Omega_i} Z_i^\beta(\mathbf{x} : \mathbf{x}_1, \dots, \mathbf{x}_N) dx + \sum_{1\leq j\neq i\leq N} \int_{\mathbf{x}\in\Omega_j} Z_i^\beta(\mathbf{x} : \mathbf{x}_1, \dots, \mathbf{x}_N) dx \tag{8}$$

$$= \int_{\mathbf{x}\in\Omega_i} \left(1 - \sum_{j\neq i} Z_j^\beta(\mathbf{x} : \mathbf{x}_1, \dots, \mathbf{x}_N)\right) dx + \sum_{j\neq i} \int_{\mathbf{x}\in\Omega_j} Z_i^\beta(\mathbf{x} : \mathbf{x}_1, \dots, \mathbf{x}_N) dx$$

$$= |\Omega_i| - \sum_{j\neq i} \int_{\mathbf{x}\in\Omega_i} Z_j^\beta(\mathbf{x} : \mathbf{x}_1, \dots, \mathbf{x}_N) dx + \sum_{j\neq i} \int_{\mathbf{x}\in\Omega_j} Z_i^\beta(\mathbf{x} : \mathbf{x}_1, \dots, \mathbf{x}_N) dx.$$

By means of Lemma 2.2, all integrals tend to zero in the limit $\beta \to +\infty$, so it proves (5). □

2.1 Partial derivatives in closed form

Now we come to the involved part of the Section, which is to show that partition functions can be used to calculate in full rigor the closed form of the partial derivatives

$$\nabla_{\mathbf{x}_k} |\Omega_i| = \lim_{\beta\to+\infty} \int_{\mathbf{x}\in\Omega} \nabla_{\mathbf{x}_k} Z_i^\beta(\mathbf{x} : \mathbf{x}_1, \dots, \mathbf{x}_N) dx. \tag{9}$$

The method of the proof is similar to the one used for showing Proposition 2.1, even if it needs more steps and is more technical.

Our notations are as follows. The $d-1$-dimensional measure of the interface between Ω_i and Ω_k is denoted as $\sigma_{ik} = \mathrm{mes}_{d-1}(\partial\Omega_i \cap \partial\Omega_k)$. The outgoing normal from Ω_i in the direction of Ω_k is $\mathbf{n}_{ik} = \frac{\mathbf{x}_k-\mathbf{x}_i}{|\mathbf{x}_k-\mathbf{x}_i|}$. The center of mass of the interface is

$$\mathbf{x}^{ik} = \mathbf{x}^{ki} = \frac{1}{\sigma_{ik}} \int_{\mathbf{x}\in\Omega_i\cap\Omega_k} \mathbf{x} d\sigma \in \partial\Omega_i \cap \partial\Omega_k.$$

Finally the mid point between $\mathbf{x}_i$ and $\mathbf{x}_k$ is denoted as $\mathbf{x}_{ik} = \mathbf{x}_{ki} = \frac{\mathbf{x}_i+\mathbf{x}_k}{2} \in \partial\Omega_i \cap \partial\Omega_k$. In dimension $d = 1$, one always has that $\mathbf{x}^{jk} = \mathbf{x}_{jk}$. The main result of the Section is as follows.

Theorem 2.3. *The derivatives of the volume $|\Omega_i|$ with respect to the generators satisfy the two properties: i) For $k \neq i$, one has the closed form formula*

$$\nabla_{\mathbf{x}_k} |\Omega_i| = \sigma_{ik} \left(\frac{\mathbf{n}_{ik}}{2} - \frac{\mathbf{x}^{ik} - \mathbf{x}_{ik}}{|\mathbf{x}_k - \mathbf{x}_i|}\right). \tag{10}$$

ii) One has the addition formula

$$\sum_{k=1}^N \nabla_{\mathbf{x}_k} |\Omega_i| = -\int_{\mathbf{x}\in\partial\Omega_i\cap\partial\Omega} \mathbf{n}(\mathbf{x}) d\sigma \tag{11}$$

where $\mathbf{n}(\mathbf{x})$ is the exterior normal from Ω.

Remark 2.4. *For $k \neq i$, the partial derivative $\nabla_{\mathbf{x}_k}|\Omega_i|$ is the sum of two orthogonal vectors. In dimension $d = 1$, the second vector always vanish and $\nabla_{\mathbf{x}_k}|\Omega_i = \pm\frac{1}{2}$ away from the boundary, a fact that we will recover directly in the one dimensional configuration (12).*

Remark 2.5. *The addition formula can be used to calculate $\nabla_{\mathbf{x}_i}|\Omega_i|$.*

Remark 2.6. *The analysis of the regularity of $|\Omega_i|$ with respect to the generators will be examined on the basis of formulas (10-11) in Corollary 2.11.*

Remark 2.7. *We illustrate the meaning of (10-11) by considering consider a simple situation in dimension $d = 1$, with the domain is $\Omega = (0, 1)$. The generators are*

$$0 < x_1 < \cdots < x_N < 1. \tag{12}$$

The Voronoï cells are the intervals $\Omega_1 = \left(0, \frac{x_1+x_2}{2}\right)$, $\Omega_i = \left(\frac{x_{i-1}+x_i}{2}, \frac{x_i+x_{i+1}}{2}\right)$ for $2 \leq i \leq N-1$, then $\Omega_N = \left(\frac{x_{N-1}+x_N}{2}, 1\right)$. The lengths are $|\Omega_1| = \frac{x_1+x_2}{2}$, $|\Omega_i| = \frac{x_{i+1}-x_{i-1}}{2}$ for $2 \leq i \leq N-1$, then $|\Omega_N| = 1 - \frac{x_{N-1}+x_N}{2}$. Three cases can be distinguished.

- *For $2 \leq i \leq N-1$, one verifies that $\partial_{x_{i+1}}|\Omega_i| = \frac{1}{2}$, $\partial_{x_{i-1}}|\Omega_i| = -\frac{1}{2}$ and $\partial_{x_k}|\Omega_i| = 0$ for $k \neq i \pm 1$. It is in accordance with the first part of the Theorem.*
- *For $i = 1$, one verifies that $\partial_{x_1}|\Omega_1| = \frac{1}{2}$, $\partial_{x_2}|\Omega_i| = \frac{1}{2}$ and $\partial_{x_k}|\Omega_i| = 0$ for $k \geq 3$. It is in accordance with the second part of the Theorem.*
- *For $i = N$, one verifies that $\partial_{x_{N-1}}|\Omega_N| = -\frac{1}{2}$, $\partial_{x_N}|\Omega_N| = -\frac{1}{2}$ and $\partial_{x_k}|\Omega_i| = 0$ for $k \leq N-2$. It is also in accordance with the second part of the Theorem.*

A separate geometrical proof of (10) in a simplified two-dimensional situation is provided in the appendix.

2.2 Proof the main Theorem 2.3

The proof of the Theorem is decomposed in several elementary steps. To calculate the gradient of the volume with respect to $\mathbf{x}_k \neq \mathbf{x}_i$, we evaluate

$$\nabla_{\mathbf{x}_k} Z_i^\beta(\mathbf{x} : \mathbf{x}_1, \ldots, \mathbf{x}_N) = -2\beta\,(\mathbf{x} - \mathbf{x}_k)\,\frac{e^{-\beta|\mathbf{x}-\mathbf{x}_i|^2} e^{-\beta|\mathbf{x}-\mathbf{x}_k|^2}}{\left(\sum_{r=1}^N e^{-\beta|\mathbf{x}-\mathbf{x}_r|^2}\right)^2}. \tag{13}$$

One has the natural decomposition

$$\int_{\mathbf{x}\in\Omega} \nabla_{\mathbf{x}_k} Z_i^\beta(\mathbf{x} : \mathbf{x}_1, \ldots, \mathbf{x}_N)dx = \int_{\mathbf{x}\in\Omega_i\cap\Omega_k} \nabla_{\mathbf{x}_k} Z_i^\beta(\mathbf{x} : \mathbf{x}_1, \ldots, \mathbf{x}_N)dx \tag{14}$$

$$+ \sum_{j\neq i \text{ and } j\neq k} \int_{\mathbf{x}\in\Omega_j} \nabla_{\mathbf{x}_k} Z_i^\beta(\mathbf{x} : \mathbf{x}_1, \ldots, \mathbf{x}_N)dx.$$

The next Lemma shows that the last integrals vanish at the limit $\beta \to \infty$.

Lemma 2.8. *There exists $C > 0$ such that if $j \neq i$ and $j \neq k$, then $\left|\int_{\mathbf{x}\in\Omega_j} \nabla_{\mathbf{x}_k} Z_i^\beta(\mathbf{x} : \mathbf{x}_1, \ldots, \mathbf{x}_N)dx\right| \leq \frac{C}{\beta}$.*

Proof. Using (13), one has the bound

$$\left|\int_{\mathbf{x}\in\Omega_j} \nabla_{\mathbf{x}_k} Z_i^\beta(\mathbf{x} : \mathbf{x}_1, \ldots, \mathbf{x}_N)dx\right| \leq 2\beta\mathrm{diam}(\Omega) \int_{\mathbf{x}\in\Omega_j} Z_i^\beta(\mathbf{x} : \mathbf{x}_1, \ldots, \mathbf{x}_N) Z_k^\beta(\mathbf{x} : \mathbf{x}_1, \ldots, \mathbf{x}_N)dx.$$

Consider the functions f_{ij} and f_{kj} defined by (7). One has

$$\int_{\mathbf{x}\in\Omega_j} Z_i^\beta(\mathbf{x} : \mathbf{x}_1, \ldots, \mathbf{x}_N) Z_k^\beta(\mathbf{x} : \mathbf{x}_1, \ldots, \mathbf{x}_N)dx \leq \int_{\mathbf{x}\in\Omega_j} e^{-\beta(f_{ij}(\mathbf{x})+f_{kj}(\mathbf{x}))}dx.$$

The claim is proved if one can obtained sharp bound on the last term. There are two cases.
In the first case, the vectors $\mathbf{x}_i - \mathbf{x}_j$ and $\mathbf{x}_k - \mathbf{x}_j$ are linearly independent as depicted in Figure 2. Then it is always possible to use a frame such that $\mathbf{x}_j = 0$, $\mathbf{x}_i - \mathbf{x}_j = (\alpha_{ij}, 0, \ldots, 0)$ is on the first axis, and $\mathbf{x}_k - \mathbf{x}_j = (\delta_{kj}, \gamma_{kj}, 0, \ldots, 0)$ belongs to the vectorial subspace spanned by the two first unit vectors. Since the vectors are linearly independent, it is also possible to make the frame such that $\alpha_{ij} > 0$ and $\gamma_{kj} > 0$. In this aligned frame, one has

$$f_{ij}(x_1, x_2, \ldots, x_N) = 2(x_1 - \alpha_{ij}/2)\alpha_{ij} \text{ and } f_{kj}(x_1, x_2, \ldots, x_N) = 2(x_1 - \delta_{kj}/2)\beta_{kj} + 2(x_2 - \gamma_{kj}/2)\gamma_{kj}.$$

By construction, one has that $\mathbf{x} \in \Omega_j \Longrightarrow f_{ij}(x_1, x_2, \ldots, x_N) \geq 0$ and $f_{kj}(x_1, x_2, \ldots, x_N) \geq 0$. So one can write

$$\int_{\mathbf{x}\in\Omega_j} e^{-\beta(f_{ij}(\mathbf{x})+f_{kj}(\mathbf{x}))}dx \leq \mathrm{diam}(\Omega)^{d-2} \int_{(x_1,x_2)\in\mathcal{Q}} e^{-2\beta((x_1-\alpha_{ij}/2)\alpha_{ij}+(x_1-\delta_{kj}/2)\beta_{kj}+2(x_2-\gamma_{kj}/2)\gamma_{kj})}dx_1dx_2$$

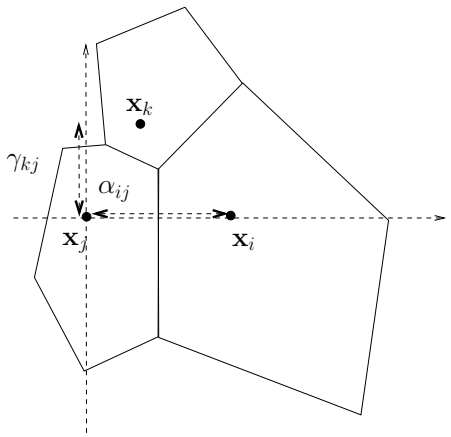

Figure 2: Three Voronoï cells with linearly independent directions $\mathbf{x}_i - \mathbf{x}_j$ and $\mathbf{x}_k - \mathbf{x}_j$. Here the cells are close neighbors, but it is not mandatory.

where $\mathcal{Q}$ is defined by

$$\mathcal{Q} = \left\{(x_1, x_2) \in \mathbb{R}^2 \text{ such that } (x_1 - \alpha_{ij}/2)\alpha_{ij} \geq 0 \text{ and } (x_1 - \delta_{kj}/2)\delta_{kj} + (x_2 - \gamma_{kj}/2)\gamma_{kj} \geq 0\right\}.$$

A natural change of variable is $u = (x_1 - \alpha_{ij}/2)\alpha_{ij}$ and $v = (x_1 - \delta_{kj}/2)\delta_{kj} + (x_2 - \gamma_{kj}/2)\gamma_{kj}$. Since $\alpha_{ij}\gamma_{kj} > 0$, the change of variable is invertible and $dudv = \alpha_{ij}\gamma_{kj}dx_1dx_2$. So one has

$$\int_{\mathbf{x}\in\Omega_j} e^{-\beta(f_{ij}(\mathbf{x})+f_{kj}(\mathbf{x}))}dx \leq \frac{\text{diam}(\Omega)^{d-2}}{\alpha_{ij}\gamma_{kj}} \int_{u>0,\ v>0} e^{-2\beta(u+v)}dudv = \frac{\text{diam}(\Omega)^{d-2}}{4\alpha_{ij}\gamma_{kj}\beta^2}. \tag{15}$$

One obtains

$$\left| \int_{\mathbf{x}\in\Omega_j} \nabla_{\mathbf{x}_k} Z_i^\beta(\mathbf{x} : \mathbf{x}_1, \ldots, \mathbf{x}_N)dx \right| \leq \frac{\text{diam}(\Omega)^{d-1}}{2\alpha_{ij}\gamma_{kj}\beta} \tag{16}$$

which is the claim for one particular value of the constant.
In the second case, the vectors $\mathbf{x}_i - \mathbf{x}_j$ and $\mathbf{x}_k - \mathbf{x}_j$ are linearly dependent so the previous method of analysis cannot work. This is illustrated in Figure 3. However it is possible once again to consider an aligned frame such

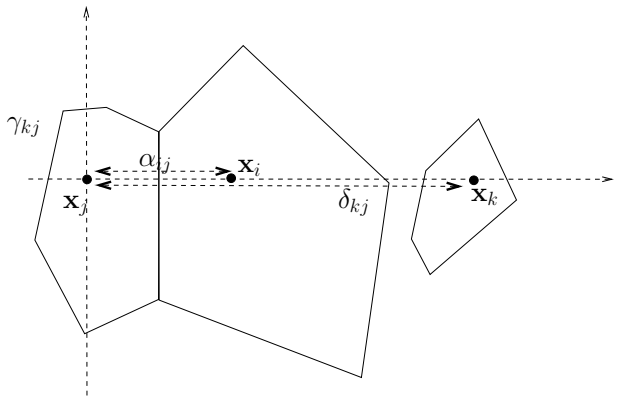

Figure 3: Example of three Voronoï cells with linearly dependent directions $\mathbf{x}_i - \mathbf{x}_j$ and $\mathbf{x}_k - \mathbf{x}_j$.

that $\mathbf{x}_j = 0$, $\mathbf{x}_i - \mathbf{x}_j = (\alpha_{ij}, 0, \ldots, 0)$ is on the first axis, and $\mathbf{x}_k - \mathbf{x}_j = (\delta_{kj}, 0, \ldots, 0)$. Since (2) holds without restriction, then $\alpha_{ij} \neq \delta_{kj}$ and one can assume that $0 < \alpha_{ij} < \delta_{kj}$. The functions write

$$f_{ij}(x_1, x_2, \ldots, x_N) = 2(x_1 - \alpha_{ij}/2)\alpha_{ij} \text{ and } f_{kj}(x_1, x_2, \ldots, x_N) = 2(x_1 - \delta_{kj}/2)\delta_{kj}.$$

For $\mathbf{x} \in \Omega_j$, then $f_{kj}(x_1, x_2, \ldots, x_N) \geq 0$ which yields $x_1 - \delta_{kj}/2 \geq 0$. Then

$$f_{ij}(x_1, x_2, \ldots, x_N) = 2(x_1 - \alpha_{ij}/2)\alpha_{ij} \geq 2(\delta_{kj}/2 - \alpha_{ij}/2)\alpha_{ij} = (\delta_{kj} - \alpha_{ij})\alpha_{ij} = |\mathbf{x}_k - \mathbf{x}_j|\alpha_{ij} > 0$$

and

$$\int_{\mathbf{x}\in\Omega_j} e^{-\beta(f_{ij}(\mathbf{x})+f_{kj}(\mathbf{x}))}dx \leq e^{-\beta|\mathbf{x}_k-\mathbf{x}_j|\alpha_{ij}} \int_{x_1>\delta_{kj}/2} e^{-\beta(2(x_1-\delta_{kj}/2)\delta_{kj}}dx \leq e^{-\beta|\mathbf{x}_k-\mathbf{x}_j|\alpha_{ij}} \frac{\text{diam}(\Omega)^{d-1}}{2\beta\delta_{kj}}. \tag{17}$$

The last inequality is non optimal but sufficient for our purposes. One obtains

$$\left|\int_{\mathbf{x}\in\Omega_j}\nabla_{\mathbf{x}_k}Z_i^\beta(\mathbf{x}:\mathbf{x}_1,\dots,\mathbf{x}_N)dx\right|\leq\frac{\mathrm{diam}(\Omega)^d}{\delta_{kj}}e^{-\beta|\mathbf{x}_k-\mathbf{x}_j|\alpha_{ij}}\leq\frac{C_{ijk}}{\beta}\tag{18}$$

for some constant $C_{ijk}>0$ because $\lim_{\beta\to+\infty}\beta e^{-\beta|\mathbf{x}_k-\mathbf{x}_j|\alpha_{ij}}=0$.

The final estimate is obtained by taking the largest constant in (16-18). □

Using Lemma 2.8, the decomposition (14) can be simplified under the form

$$\int_{\mathbf{x}\in\Omega}\nabla_{\mathbf{x}_k}Z_i^\beta(\mathbf{x}:\mathbf{x}_1,\dots,\mathbf{x}_N)dx=\int_{\mathbf{x}\in\Omega_i\cup\Omega_k}\nabla_{\mathbf{x}_k}Z_i^\beta(\mathbf{x}:\mathbf{x}_1,\dots,\mathbf{x}_N)+O(\beta^{-1}).$$

We continue the analysis by simplifying the term under the integral as much as possible, until a direct calculation of the limit $\beta\to+\infty$ is possible. We will use the simplified notation $\alpha_i:=e^{-\beta|\mathbf{x}-\mathbf{x}_i|^2}$. Considering (13), one can write

$$\nabla_{\mathbf{x}_k}Z_i^\beta(\mathbf{x}:\mathbf{x}_1,\dots,\mathbf{x}_N)=2\beta\,(\mathbf{x}-\mathbf{x}_k)\,\frac{e^{-\beta|\mathbf{x}-\mathbf{x}_i|^2}e^{-\beta|\mathbf{x}-\mathbf{x}_k|^2}}{\left(e^{-\beta|\mathbf{x}-\mathbf{x}_i|^2}+e^{-\beta|\mathbf{x}-\mathbf{x}_k|^2}\right)^2}+R_{ik}(\mathbf{x})\tag{19}$$

where the residual $R_{ik}(\mathbf{x})$ is

$$R_{ik}(\mathbf{x})=2\beta\,(\mathbf{x}-\mathbf{x}_k)\,(\alpha_i\alpha_k)\left(\frac{1}{\left(\sum_{r=1}^N\alpha_r\right)^2}-\frac{1}{(\alpha_i+\alpha_k)^2}\right)$$

$$=-2\beta\,(\mathbf{x}-\mathbf{x}_k)\,(\alpha_i\alpha_k)\left(\frac{1}{\sum_{r=1}^N\alpha_r}+\frac{1}{(\alpha_i+\alpha_k)}\right)\frac{\sum_{r\neq k,\ r\neq i}\alpha_r}{(\alpha_i+\alpha_k)\left(\sum_{r=1}^N\alpha_r\right)}.$$

One has the preparatory inequality $|R_{ik}(\mathbf{x})|\leq 4\beta\mathrm{diam}(\Omega)\frac{\alpha_i\alpha_k}{(\alpha_i+\alpha_k)^2}\times\sum_{r\neq k,\ r\neq i}\frac{\alpha_r}{\sum_{s=1}^N\alpha_s}$.

Lemma 2.9. *There exists $C>0$ such that $\left|\int_{\mathbf{x}\in\Omega_i\cup\Omega_k}R_{ik}(\mathbf{x})dx\right|\leq\frac{C}{\beta}$ for all indices $1\leq i,k\leq N$.*

Proof. We firstly consider the integral $\int_{\mathbf{x}\in\Omega_i}R_{ik}(\mathbf{x})dx$. One has the bound

$$|R_{ik}(\mathbf{x})|\leq 4\beta\mathrm{diam}(\Omega)\frac{\alpha_k}{\alpha_i}\times\sum_{r\neq k,\ r\neq i}\frac{\alpha_r}{\alpha_i}=4\beta\mathrm{diam}(\Omega)\sum_{r\neq k,\ r\neq i}e^{-\beta(f_{ji}(\mathbf{x})+f_{ri}(\mathbf{x}))}$$

where f_{ji} and f_{ri} are defined by (7). It is sufficient to use (15-17) to obtain $\left|\int_{\mathbf{x}\in\Omega_i}R_{ik}(\mathbf{x})\right|\leq C/\beta$. Similarly $\left|\int_{\mathbf{x}\in\Omega_k}R_{ik}(\mathbf{x})\right|\leq C/\beta$, which ends the proof. □

So one can write

$$\int_{\mathbf{x}\in\Omega}\nabla_{\mathbf{x}_k}Z_i^\beta(\mathbf{x}:\mathbf{x}_1,\dots,\mathbf{x}_N)dx=-2\beta\int_{\mathbf{x}\in\Omega_i\cap\Omega_k}(\mathbf{x}-\mathbf{x}_k)\,\frac{e^{-\beta|\mathbf{x}-\mathbf{x}_i|^2}e^{-\beta|\mathbf{x}-\mathbf{x}_k|^2}}{\left(e^{-\beta|\mathbf{x}-\mathbf{x}_i|^2}+e^{-\beta|\mathbf{x}-\mathbf{x}_k|^2}\right)^2}dx+O(\beta^{-1}).\tag{20}$$

Now that the main contribution is isolated in the above expression of the gradient, one can end the proof of the Theorem.

Proof of the first part of Theorem 2.3. What we need to obtain is the limit (9) and of course we use (20). Let us use the translation-rotation of the frame so that one has $\frac{\mathbf{x}_i+\mathbf{x}_k}{2}=0$, $\mathbf{x}_i=(-\alpha/2,0,\dots,0)$, $\mathbf{x}_k=(\alpha/2,0,\dots,0)$ and $\alpha=|\mathbf{x}_i-\mathbf{x}_k|$. We illustrate in Figure 4 a situation where the Voronoï cells have a non trivial interface, but the situation can be the degenerated one of Figure 1 as well. We write $\mathbf{x}=(x_1,\mathbf{y})$ with $\mathbf{y}\in\mathbb{R}^{d-1}$, so $|\mathbf{x}-\mathbf{x}_i|^2=|x_1+\alpha/2|^2+|\mathbf{y}|^2$ and $|\mathbf{x}-\mathbf{x}_k|^2=|x_1-\alpha/2|^2+|\mathbf{y}|^2$. Therefore one has the simplication

$$\frac{e^{-\beta|\mathbf{x}-\mathbf{x}_i|^2}e^{-\beta|\mathbf{x}-\mathbf{x}_k|^2}}{\left(e^{-\beta|\mathbf{x}-\mathbf{x}_i|^2}+e^{-\beta|\mathbf{x}-\mathbf{x}_k|^2}\right)^2}=\frac{e^{-2\beta(x_1^2+\alpha^2/4)}}{\left(e^{-\beta(x_1^2-x_1\alpha+\alpha^2/4)}+e^{-\beta(x_1^2+x_1\alpha+\alpha^2/4)}\right)^2}=\frac{1}{\left(e^{-\beta x_1\alpha}+e^{\beta x_1\alpha}\right)^2}$$

Then the integral in the right hand side of (20) is expressed as

$$I=-2\beta\int_{\mathbf{x}\in\Omega_i\cap\Omega_k}(x_1-\alpha/2,\mathbf{y})\,\frac{1}{\left(e^{-\beta x_1\alpha}+e^{\beta x_1\alpha}\right)^2}dx_1dy.$$

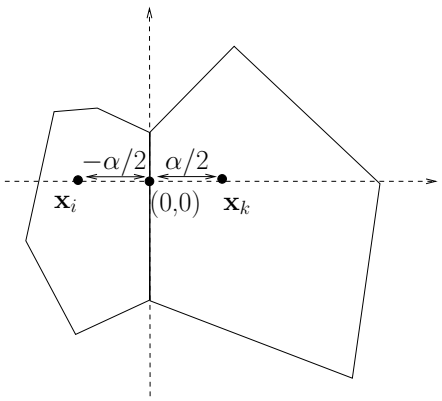

Figure 4: Example of two neighboring Voronoï cells.

Let us perform the change of variable $\beta x_1 = \overline{x}_1$. One obtains

$$I = -2 \int_{(\overline{x}_1/\beta, \mathbf{y}) \in \Omega_i \cap \Omega_k} (\overline{x}_1/\beta - \alpha/2, \mathbf{y}) \, \frac{1}{\left(e^{-\overline{x}_1 \alpha} + e^{\overline{x}_1 \alpha}\right)^2} d\overline{x}_1 dy$$

which can be decomposed as $I = I_1 + I_2$ where

$$I_1 = -\frac{2}{\beta} \int_{(\overline{x}_1/\beta, \mathbf{y}) \in \Omega_i \cap \Omega_k} (\overline{x}_1, \mathbf{0}) \, \frac{1}{\left(e^{-\overline{x}_1 \alpha} + e^{\overline{x}_1 \alpha}\right)^2} d\overline{x}_1 dy$$

and

$$I_2 = -2 \int_{(\overline{x}_1/\beta, \mathbf{y}) \in \Omega_i \cap \Omega_k} (-\alpha/2, \mathbf{y}) \, \frac{1}{\left(e^{-\overline{x}_1 \alpha} + e^{\overline{x}_1 \alpha}\right)^2} d\overline{x}_1 dy$$

Lemma 2.10. *There exists a constant $C > 0$ such that $I_1 \leq \frac{C}{\beta}$.*

Proof. One notices that one has the embedding $(\overline{x}_1/\beta, \mathbf{y}) \in \Omega_i \cap \Omega_k \Longrightarrow (\overline{x}_1/\beta, \mathbf{y}) \in \Omega \Longrightarrow \frac{|\overline{x}_1|^2}{\beta^2} + |\mathbf{y}|^2 \leq R^2$ for some radius $R > 0$ (which depends on Ω only). Moreover the weight inside the integrals $\frac{1}{(e^{-\overline{x}_1 \alpha} + e^{\overline{x}_1 \alpha})^2} = \frac{1}{4\alpha} \tanh'(\overline{x}_1 \alpha)$ is integrable over $\mathbb{R}$. It shows $|I_1| \leq \frac{2}{\beta} \int_{|\mathbf{y}|<R} dy \times \int_{\overline{x}_1 \in \mathbb{R}} \frac{|\overline{x}_1|}{(e^{-\overline{x}_1 \alpha} + e^{\overline{x}_1 \alpha})^2} d\overline{x}_1 \leq \frac{C}{\alpha^2 \beta} \overset{\beta \to \infty}{\longrightarrow} 0.$ □

Therefore the claim is proved provided we calculate the limit of I_2. Our method of analysis if to determine the formal limit of I_2 (this is an easy task), then to compare I_2 with its formal limit. Let us decompose the separating hyperplane between the interface and its complementary part

$$\Sigma = \partial\Omega_i \cap \partial\Omega_k \text{ and } \widehat{\Sigma} = \{\overline{x}_1 = 0\}/\Sigma.$$

This is illustrated in Figure 5. The separating hyperplane is $\{\overline{x}_1 = 0\}$ with $\Sigma \subset \{\overline{x}_1 = 0\}$. We decompose

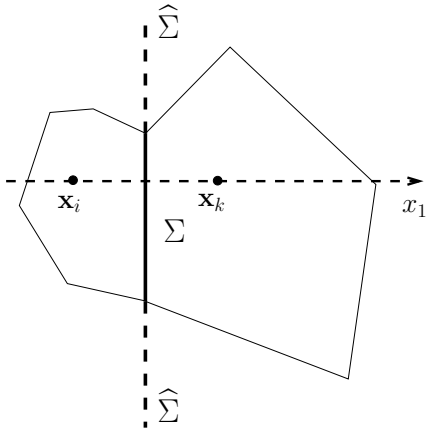

Figure 5: Decomposition of the separating hyperplane $\{\overline{x}_1 = 0\} = \Sigma \cup \widehat{\Sigma}$ between two Voronoï cells.

$I_2 = I_3 + I_4$ where of I_3 is evaluated with respect to the complementary part of the interface

$$I_3 = -2 \int_{(0,\mathbf{y}) \in \widehat{\Sigma}} \left(\int_{(\overline{x}_1/\beta, \mathbf{y}) \in \Omega_i \cap \Omega_k} \frac{(-\alpha/2, \mathbf{y})}{\left(e^{-\overline{x}_1 \alpha} + e^{\overline{x}_1 \alpha}\right)^2} d\overline{x}_1 \right) dy$$

and I_4 is evaluated with respect to the interface

$$I_4 = -2\int_{(0,\mathbf{y})\in\Sigma}\left(\int_{(\overline{x}_1/\beta,\mathbf{y})\in\Omega_i\cap\Omega_k}\frac{(-\alpha/2,\mathbf{y})}{\left(e^{-\overline{x}_1\alpha}+e^{\overline{x}_1\alpha}\right)^2}d\overline{x}_1\right)dy.$$

• Let us firstly consider I_3. One can use Lemma 2.14 since the exterior integral si over $\widehat{\Sigma}$. One gets that for almost all $\mathbf{y}\in\widehat{\Sigma}$, one has that $(\overline{x}_1/\beta,\mathbf{y})\in\Omega_i\cap\Omega_k$ implies that $|\overline{x}_1|/\beta\geq\varepsilon>0$ where ε depends on h. Therefore

$$\left|\int_{(\overline{x}_1/\beta,\mathbf{y})\in\Omega_i\cap\Omega_k}\frac{(-\alpha/2,\mathbf{y})}{\left(e^{-\overline{x}_1\alpha}+e^{\overline{x}_1\alpha}\right)^2}d\overline{x}_1\right|\leq C\int_{\overline{x}_1>\varepsilon\beta}\frac{1}{\left(e^{-\overline{x}_1\alpha}+e^{\overline{x}_1\alpha}\right)^2}d\overline{x}_1\underset{\beta\to+\infty}{\longrightarrow}0\quad\text{for almost all }\mathbf{y}\in\widehat{\Sigma}.\tag{21}$$

Moreover this term is bounded uniformly with respect to $\mathbf{y}$. It is null for $|\mathbf{y}|$ large enough because Ω is bounded by hypothesis. Then the Lebesgue's dominated convergence Theorem yields that

$$\lim_{\beta\to+\infty}I_3=0.$$

• Next we consider I_4. Its formal limit is

$$I_4^\infty=-2\int_{(0,\mathbf{y})\in\Sigma}\left(\int_{\overline{x}_1\in\mathbb{R}}\frac{(-\alpha/2,\mathbf{y})}{\left(e^{-\overline{x}_1\alpha}+e^{\overline{x}_1\alpha}\right)^2}d\overline{x}_1\right)dy=\frac{1}{\alpha}\int_{(0,\mathbf{y})\in\partial\Omega_i\cap\partial\Omega_k}(\alpha/2,-\mathbf{y})\,dy$$

by exact integration of the weight. The difference between the integral and its formal limit is

$$I_4-I_4^\infty=-2\int_{(0,\mathbf{y})\in\Sigma}\left(\int_{\overline{x}_1\in\mathbb{R}}\left(\mathbf{1}_{(\overline{x}_1/\beta,\mathbf{y})\in\Omega_i\cap\Omega_k}-1\right)\frac{(-\alpha/2,\mathbf{y})}{\left(e^{-\overline{x}_1\alpha}+e^{\overline{x}_1\alpha}\right)^2}d\overline{x}_1\right)dy$$

To prove the difference tends to zero, we use Lemma 2.13 which shows that $\mathbf{1}_{(\overline{x}_1/\beta,\mathbf{y})\in\Omega_i\cap\Omega_k}-1\to0$ for almost all $\mathbf{y}$ such that $(0,\mathbf{y})\in\Sigma$ and almost all $\overline{x}_1\in\mathbb{R}$. Therefore

$$\int_{\overline{x}_1\in\mathbb{R}}\left(\mathbf{1}_{(\overline{x}_1/\beta,\mathbf{y})\in\Omega_i\cap\Omega_k}-1\right)\frac{(-\alpha/2,\mathbf{y})}{\left(e^{-\overline{x}_1\alpha}+e^{\overline{x}_1\alpha}\right)^2}d\overline{x}_1\underset{\beta\to+\infty}{\longrightarrow}0\quad\text{for almost all }\mathbf{y}\in\Sigma.\tag{22}$$

By integration over Σ, one gets by invoking the Lebesgue's dominated convergence Theorem that $\lim_{\beta\to+\infty}I_4=I_4^\infty$. Let us denote $\mathbf{n}=\frac{\mathbf{x}_k-\mathbf{x}_j}{|\mathbf{x}_k-\mathbf{x}_j|}$ such that $\mathbf{n}=(1,0,\ldots,0)$ in the new frame. One gets $I_4^\infty=\frac{1}{2}\int_{(0,\mathbf{y})\in\Omega_i\cap\Omega_k}dy\,\mathbf{n}-\frac{1}{\alpha}\int_{(0,\mathbf{y})\in\Omega_i\cap\Omega_k}\mathbf{y}dy$. Using the fact that $\frac{\mathbf{x}_i+\mathbf{x}_k}{2}=0$ in the adapted frame, we rewrite thus expression as $I_4^\infty=\frac{1}{2}\mathbf{n}\sigma-\int_{\mathbf{x}\in\Omega_i\cap\Omega_k}\frac{\mathbf{x}-\frac{\mathbf{x}_i+\mathbf{x}_k}{2}}{\alpha}d\sigma$. With the notations used in Theorem 2.3, this is the first claim (10). □

Proof of the second part of Theorem 2.3. Let us assume that all generators move in a uniform translation, that is $\frac{d}{dt}\mathbf{x}_k(t)=\mathbf{a}\in\mathbb{R}^d$ for $1\leq k\leq N$. Since the Voronoï cell moves with the same velocity, its volume of a Voronoï cell away from the boundary is constant in time $\left\langle\sum_{k=1}^N\nabla_{\mathbf{x}_k}|\Omega_i|,\mathbf{a}\right\rangle=0$ for all velocity vector $\mathbf{a}\in\mathbb{R}^d$. It yields $\sum_{k=1}^N\nabla_{\mathbf{x}_k}|\Omega_i|=0$. The general case is that the Voronoï cell shares a part of the exterior boundary of Ω. Then, when all generators move with the same velocity vector $\mathbf{a}\in\mathbb{R}^d$, the volume evolves with the law $\frac{d}{dt}|\Omega_i|=-\int_{\mathbf{x}\in\partial\Omega_i\cap\partial\Omega}\langle\mathbf{n}(\mathbf{x}),\mathbf{a}\rangle\,d\sigma$ that is

$$\left\langle\sum_{k=1}^N\nabla_{\mathbf{x}_k}|\Omega_i|,\mathbf{a}\right\rangle=-\int_{\mathbf{x}\in\partial\Omega_i\cap\partial\Omega}\langle\mathbf{n}(\mathbf{x}),\mathbf{a}\rangle\,d\sigma.$$

Since it holds for all $\mathbf{a}\in\mathbb{R}^d$, it proves the second part of the Theorem. □

Corollary 2.11. *The volume $|\Omega_i|$ is locally Lipschitz with respect to the generators.*

Proof. The formulas (10-11) show that the partial derivatives are bounded in maximal norm provided the generators are not too close, that is provided $|\mathbf{x}_k-\mathbf{x}_j|\geq\varepsilon>0$ for some constant $\varepsilon>0$ which can be as small as desired. So the volume $|\Omega_i|$ is locally Lipshitz. □

Remark 2.12. *Since the geometrical elements visible in the right hand side in (10) are naturally continuous with respect to the generators, one can anticipate that the regularity of the volume is generically C^1 with respect to the generators. However it is not completely clear that the right hand side in (11) is also continuous with respect to the generators, for example if a Voronoï cell touches the boundary $\partial\Omega$. We leave this issue for further research.*

2.3 Proof of the technical results (21) and (22)

The notations are the one of Figure 5 and we note $\mathbf{n}$ the outgoing normal from Ω_j. We assume that $\mathbf{n}$ is aligned with the first axis, that is $\mathbf{n} = (1, 0, \ldots, 0)$.

Lemma 2.13 (Proof of (21))**.** *For almost all* $\mathbf{y}$ *such that* $(0, \mathbf{y}) \in \Sigma$*, there exists* $\varepsilon > 0$ *such that for all* $h \in (-\varepsilon, \varepsilon)$*, then one has* $\mathbf{y} + h\mathbf{n} \in \Omega_j \cup \Omega_k$*.*

Proof. Since Ω_i and Ω_k are Voronoi cells embedded in Ω which is a polytope by hypothesis, then the interface $\Sigma \subset \{\overline{x}_1 = 0\}$ is a $d-1$ dimensional polytope. For $\mathbf{y} \in \mathbb{R}^{d-1}$, we will note the $d-1$ dimensional sphere $S_\varepsilon(\mathbf{y}) = \{\mathbf{z} \in \mathbb{R}^{d-1} \text{ such that } |\mathbf{z} - \mathbf{y}| < \varepsilon\}$.

Now for almost all $\mathbf{y}$ such that $(0, \mathbf{y}) \in \Sigma$, there exists $\varepsilon > 0$ small enough such that $z \in S_\varepsilon(\mathbf{y}) \Longrightarrow (0, \mathbf{z}) \in \Sigma$. Consider all points obtained by linear interpolation between $(0, \mathbf{z})$ and $\mathbf{x}_j$

$$\alpha(0, \mathbf{z}) \ + (1 - \alpha)\mathbf{x}_i \in \Omega_j \text{ for } 0 \leq \alpha < 1.$$

The idea is to look for a pair $(\mathbf{z}, \alpha) \in \mathbf{R}^{d-1} \times \mathbf{R}$ such that

$$\alpha(0, \mathbf{z}) \ + (1 - \alpha)\mathbf{x}_j = (\mu, \mathbf{y}) \text{ for some } \mu \neq 0.$$

To solve this problem we use the decomposition $\mathbf{x}_j = (\gamma, \mathbf{w})$ with $\gamma \neq 0$ (since $\mathbf{x}_j$ is in the interior of the Voronoï cell) and substitute. We find the linear system

$$\begin{cases} \mu = (1 - \alpha)\gamma, \\ \mathbf{y} = \alpha\mathbf{z} + (1 - \alpha)\mathbf{w}. \end{cases}$$

In the case $\mathbf{w} = \mathbf{y}$, a solution is $\alpha = 0$ and $\mu = \gamma$.
In the case $\mathbf{w} \neq \mathbf{y}$, a natural solution is obtained by taking $\mathbf{z} = \mathbf{y} - \frac{\varepsilon}{2} \times \frac{\mathbf{w}-\mathbf{y}}{|\mathbf{w}-\mathbf{y}|}$ and $\alpha = \frac{|\mathbf{w}-\mathbf{y}|}{\frac{\varepsilon}{2}+|\mathbf{w}-\mathbf{y}|}$. The construction is illustrated in Figure 6. It yields $\mu = \frac{\varepsilon\gamma}{\varepsilon+2|\mathbf{w}-\mathbf{y}|}$. Since $(0, \mathbf{z}) \in \Omega_i$ and $\mathbf{x}_i \in \Omega_i$ one has by

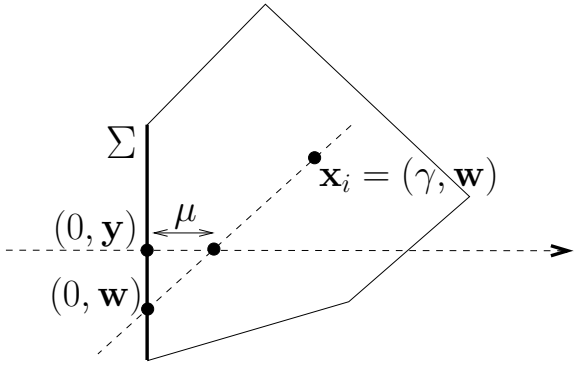

Figure 6: Illustration of Lemma 21. For almost points $(0, \mathbf{y}) \in \Sigma$, there exists a non zero interval/segment *pointing inward in the normal direction* which belongs to Ω_i.

convexity $(\mu, \mathbf{y}) = (0, \mathbf{y}) + \mu\mathbf{n} \in \Omega_i$. So by convexity,

$$(0, \mathbf{y}) + h\mathbf{n} \in \Omega_i \text{ for all } 0 < h < \mu.$$

Doing the same analysis on the other side, that is in Ω_k, one gets a similar result

$$(0, \mathbf{y}) - h\mathbf{n} \in \Omega_j \text{ for all } 0 < h < \widetilde{\mu}.$$

The claim is obtained with $\varepsilon = \min(\mu, \widetilde{\mu}) > 0$. □

Lemma 2.14 (Proof of (22))**.** *For almost all* $\mathbf{y}$ *such that* $(0, \mathbf{y}) \in \{\overline{x}_1 = 0\}/\Sigma$*, there exists* $\varepsilon > 0$ *such that for all* $h \in (-\varepsilon, \varepsilon)$*, then one has* $\mathbf{y} + h\mathbf{n} \notin \Omega_i \cup \Omega_k$*.*

Proof. The proof is by contradiction. We start by assuming the statement: *there exists* $\mathbf{y}$ *such that* $(0, \mathbf{y}) \in \{\overline{x}_1 = 0\}/\Sigma$ *and dist*$(\mathbf{y}, \partial\Omega_i \cap \partial\Omega_k) > 0$ *and a sequence* $\mathbf{w}_n = \mathbf{y} + h_n\mathbf{n} \in \Omega_i \cup \Omega_k$ *which satisfies* $h_n \to 0$*.*

If this statement is true then, passing to the limit, one obtains that $\mathbf{y} \in \partial\Omega_i \cap \partial\Omega_k$. Since $\mathbf{y}$ belongs to the separating hyperplane, then $\text{dist}(\mathbf{y}, \partial\Omega_i \cap \partial\Omega_k) = 0$ which is in contradiction with the statement. So the opposite statement holds: *for all* $\mathbf{y}$ *such that* $(0, \mathbf{y}) \in \{\overline{x}_1 = 0\}/\Sigma$ *and dist*$(\mathbf{y}, \partial\Omega_i \cap \partial\Omega_k) > 0$*, then there exists* $\varepsilon > 0$ *such that* $\mathbf{w} = \mathbf{y} + h\mathbf{n} \notin \Omega_i \cup \Omega_k$ *for* $|h| < \varepsilon$*.* It yields the claim. □

3 An application to lagrangian particle dynamics

We show in this Section that lagrangian Voronoï meshes can be used to define new numerical methods for the discretization of fluid mechanics equations. These numerical methods can be seen as particles methods since the mass of the particles is constant. The model problem is the system of compressible non viscous Euler equations with entropy inequality

$$\left\{\begin{array}{l} \partial_t \rho + \nabla \cdot (\rho \mathbf{u}) = 0, \\ \partial_t \rho \mathbf{u} + \nabla \cdot (\rho \mathbf{u} \otimes \mathbf{u}) + \nabla p = 0, \\ \partial_t \rho e + \nabla \cdot (\rho \mathbf{u} e + p\mathbf{u}) = 0, \\ \partial_t \rho S + \nabla \cdot (\rho \mathbf{u} S) \geq 0, \end{array}\right. \tag{23}$$

written in a bounded domain $\Omega \subset \mathbb{R}^d$. We use a perfect pressure law $p = (\gamma - 1)\rho\left(e - \frac{1}{2}|\mathbf{u}|^2\right)$ with $\gamma > 1$. The entropy inequality in the sense of distributions allows for a consistent mathematical treatment of shocks [20, 9]. The problem is equipped with a sliding condition (Neumann boundary condition)

$$\langle \mathbf{u}, \mathbf{n} \rangle = 0 \text{ for } \mathbf{x} \in \partial\Omega \tag{24}$$

where $\mathbf{n}$ is the exterior norm.

In this Section we reproduce the construction principles of the GLACE scheme [14, 7, 12] where the whole construction relies on the derivative of the volume with respect to some control points. In a more classical finite volume scheme, the control points are the vertices of the mesh. In the present work the control points are the generators/particles and the derivatives are given by Theorem 2.3. We will use the compact notation

$$\mathbf{C}_{ik} = \nabla_{\mathbf{x}_k} |\Omega_i|. \tag{25}$$

3.1 Semi-discrete scheme

The dependance with respect to the time is continuous, the time discrete scheme will be presented later. One starts with a moving lagrangian Voronoï cell $t \mapsto \Omega_j(\mathbf{x}_1(t), \ldots, \mathbf{x}_N(t))$. The lagrangian mass of the cell is constant

$$M_j = |\Omega_j(t)|\rho_j(t) \text{ is constant with respect to } t. \tag{26}$$

The inverse of the density $\rho_j(t) > 0$ is noted $\tau_j(t) = \rho_j(t)^{-1}$. The classical lagrangian integral form of (23) for all $1 \leq j \leq N$

$$\left\{\begin{array}{l} M_j \frac{d}{dt}\tau_j(t) = \int_{\partial\Omega_j(t)} \langle \mathbf{u}, \mathbf{n} \rangle \, d\sigma, \\ M_j \frac{d}{dt}\mathbf{u}_j(t) = -\int_{\partial\Omega_j(t)} p\mathbf{n} d\sigma, \\ M_j \frac{d}{dt} e_j(t) = -\int_{\partial\Omega_j(t)} p \langle \mathbf{u}, \mathbf{n} \rangle \, d\sigma, \\ M_j \frac{d}{dt} S_j(t) \geq 0, \end{array}\right. \tag{27}$$

is based on integration in cells. In our case, we discretize (4) under the form

$$M_i \frac{d}{dt}\tau_i(t) = \sum_{k=1}^{N} \langle \mathbf{C}_{ik}, \mathbf{v}_k \rangle \tag{28}$$

where $\mathbf{v}_k = \frac{d}{dt}\mathbf{x}_k$ is the velocity of the generator, which is of course still an unknown at this stage of the analysis. In this construction a difference of velocities is possible, that is $\mathbf{v}_k \neq \mathbf{u}_k$ (a similar principle is used in [32]). Clearly $\sum_{k=1}^{N} \langle \mathbf{C}_{ik}, \mathbf{v}_k \rangle$ is a discretization of the term $\int_{\partial\Omega_j(t)} \langle \mathbf{v}, \mathbf{n} \rangle \, d\sigma = \int_{\Omega_j} \nabla \cdot \mathbf{u} dx$, so it contains a discrete representation of the divergence operator. One notices that $\int_{\partial\Omega_j(t)} p\mathbf{n} d\sigma = \int_{\Omega_j} \nabla p dx$ contains a discretization of the gradient operator ∇. This analogy is already used in the GLACE scheme. We reproduce the analogy hereafter under the form

$$M_i \frac{d}{dt}\mathbf{u}_i(t) = -\sum_{k=1}^{N} \mathbf{C}_{ik} p_{ik}, \tag{29}$$

where the discrete pressure gradient in the right hand side depends on pressures p_{ik} which are still unknowns at this stage of the construction. Then the equation of the total energy is the natural formal consequence

$$M_i \frac{d}{dt} e_i(t) = -\sum_{k=1}^{N} \langle \mathbf{C}_{ik}, \mathbf{v}_k \rangle \, p_{ik}. \tag{30}$$

One obtains the system of ODEs (28-29-30). This system is not closed so far since the quantities $\mathbf{v}_k$ and p_{ik} are still unknowns. It is the role of the closure relations to provide a value for these quantities. We distinguish two cases. In the first case, the Voronoï cell shares no boundary with Ω, which means that it is strictly inside Ω. In the second case, the Voronoï shares a part of its boundary with Ω, and we will use the sliding condition (24) to close the system.

3.1.1 Closure in the general case

The closure is based on two principles widely used in cell centered finite volume discretization of (27). The first principle is to use an acoustic Godunov solver [14, 7, 12, 27, 26] written under the form of a linear relation between p_i, p_{ik}, $\mathbf{u}_i$ and $\mathbf{v}_k$

$$p_{ik} - p_i + \lambda_{ik} \left\langle \mathbf{v}_k - \mathbf{u}_i, \frac{\mathbf{C}_{ik}}{|\mathbf{C}_{ik}|} \right\rangle = 0 \tag{31}$$

where $\lambda_{ik} > 0$ is a local value of the impedance $\lambda \approx \left(\frac{\partial p}{\partial \rho|S}\right)^{\frac{1}{2}}$. For a complete specification of the scheme proposed in this work, we will take (other values are possible)

$$\lambda_{ik} = \rho_i c_i. \tag{32}$$

Acoustic Godunov solvers are known to be well adapted for discrete shock calculations even if they are basically first order only. Considering that the Voronoï cell is strictly inside of the domain (it is the general case), we postulate that $\mathbf{C}_{ik}p_{ik}$ is some kind of force exchanged between Ω_i and Ω_k. Writing that the sum of internal forces vanishes at the point $\mathbf{x}_k$ yields the linear relation the equation

$$\sum_{i=1}^{N} \mathbf{C}_{ik}p_{ik} = 0 \quad \text{for all } k, \tag{33}$$

where many terms vanish in this expression for the pairs (i,k) which have no interaction ($\mathbf{C}_{ik} = 0$). The solution is the linear system (31-33) is easy to obtain. One eliminates the pressure terms in (33) and gets

$$\left(\sum_{i=1}^{N} \lambda_{ik} \frac{\mathbf{C}_{ik} \otimes \mathbf{C}_{ik}}{|\mathbf{C}_{ik}|}\right) \mathbf{v}_k = \sum_{i=1}^{N} \mathbf{C}_{ik} \left(p_i - \lambda_{ik} \left\langle \mathbf{u}_i, \frac{\mathbf{C}_{ik}}{|\mathbf{C}_{ik}|} \right\rangle\right) \quad \text{for all } k. \tag{34}$$

Under normal conditions on the mesh, the matrix of the linear is symmetric positive, so is non singular. One can calculate the velocity $\mathbf{v}_k$. Then one calculates the pressure p_{ik} with (31).

Remark 3.1. *This procedure is the direct generalization of the corner system in GLACE or EUCCLHYD, refer to [14, 7, 12, 27, 26].*

3.1.2 Closure near the boundary

Here we generalize the analysis made in GLACE for a Voronoï cell Ω_k near the boundary such that $\partial\Omega_k \cap \partial\Omega \neq \emptyset$ has a positive $d-1$ measure. For the simplicity of the exposure, let us assume that $\partial\Omega_k \cap \partial\Omega \neq \emptyset$ is a flat boundary. It is clear on mechanical grounds that the sliding condition (24) induces a mechanical reaction of the boundary in the direction normal to the boundary. How we use this interpretation is described below.

Firstly the acoustic relations (31) remain unchanged. Secondly we consider that an exterior force is produced by the boundary on the direction normal to the boundary. We write

$$\sum_{i=1}^{N} \mathbf{C}_{ik}p_{ik} + \mathbf{C}_{\text{ext},k}p_{\text{ext},k} = 0 \tag{35}$$

where $\mathbf{C}_{\text{ext},k} = \int_{\mathbf{x}\in\partial\Omega_i\cap\partial\Omega} \mathbf{n}(\mathbf{x})d\sigma$. The exterior pressure p_{ext} is an additional unknown. Since there is an additional unknown, we need an additional linear equation. We consider the discrete sliding condition

$$\langle \mathbf{v}_k, \mathbf{n}_{\text{ext},k} \rangle = 0, \qquad \mathbf{n}_{\text{ext},k} = \frac{\mathbf{C}_{\text{ext},k}}{|\mathbf{C}_{\text{ext},k}|}. \tag{36}$$

The linear system (31-35-36) has a unique solution under normal conditions on the mesh.

To prove this fact, we consider the homogeneous linear system made of (35-36) and of the homogeneous version of (31) $p_{ik} + \lambda_{ik} \left\langle \mathbf{v}_k - \mathbf{u}_i, \frac{\mathbf{C}_{ik}}{|\mathbf{C}_{ik}|} \right\rangle = 0$. Indeed one deduces from (35) that $(I - \mathbf{n}_{\text{ext},k} \otimes \mathbf{n}_{\text{ext},k}) \sum_{i=1}^{N} \mathbf{C}_{ik}p_{ik} = 0$. Elimination of the pressures yields $(I - \mathbf{n}_{\text{ext},k} \otimes \mathbf{n}_{\text{ext},k}) \left(\sum_{i=1}^{N} \lambda_{ik} \frac{\mathbf{C}_{ik}\otimes\mathbf{C}_{ik}}{|\mathbf{C}_{ik}|}\right) \mathbf{v}_k = 0$. Since the solution $\mathbf{v}_k$ is sought in the subspace which is orthogonal to the normal vector, one has $\mathbf{v}_k = (I - \mathbf{n}_{\text{ext},k} \otimes \mathbf{n}_{\text{ext},k}) \mathbf{v}_k$. One obtains $\left[(I - \mathbf{n}_{\text{ext},k} \otimes \mathbf{n}_{\text{ext},k}) \left(\sum_{i=1}^{N} \lambda_{ik} \frac{\mathbf{C}_{ik}\otimes\mathbf{C}_{ik}}{|\mathbf{C}_{ik}|}\right) (I - \mathbf{n}_{\text{ext},k} \otimes \mathbf{n}_{\text{ext},k}) + \mathbf{n}_{\text{ext},k} \otimes \mathbf{n}_{\text{ext},k}\right] \mathbf{v}_k = 0$. The matrix is symmetric and positive under standard conditions on the mesh, so $\mathbf{v}_k = 0$ which shows that the linear system (31-35-36) has a unique solution.

3.1.3 Conservation properties and entropy inequality

In this Section, we show that the fundamental conservation properties, which allow a sound mathematical treatment [20, 9] of weak solutions with shocks and contact discontinuities, are satisfied.

Since the mass of the individual cells is lagrangian, then the total mass is preserved. The total impulse cannot be exactly preserved because of the exterior pressure terms (35). However it is locally preserved.

Lemma 3.2. *The total impulse is preserved (up to boundary contributions).*

Proof. The proof is a consequence of (35). Indeed one obtains $\frac{d}{dt}\sum_{i=1}^N M_i\mathbf{u}_i(t) = -\sum_{i=1}^N\sum_{k=1}^N \mathbf{C}_{ik}p_{ik} = -\sum_{k=1}^N\sum_{i=1}^N \mathbf{C}_{ik}\ p_{ik} = \sum_{k=1}^N \mathbf{C}_{\text{ext},k}p_{\text{ext}}$ where by convention $\mathbf{C}^n_{\text{ext},k} = 0$ is the Voronoï cell Ω_k is strictly in the interior of the domain. The last term is a discrete integral on the boundary, so the proof is ended. □

On the other hand the total energy is exactly preserved.

Lemma 3.3. *The total energy is preserved.*

Proof. One has $\frac{d}{dt}\sum_{i=1}^N M_ie_i(t) = -\sum_{j=1}^N\sum_{k=1}^N \langle\mathbf{C}_{ik},\mathbf{v}_k\rangle\, p_{ik} = -\sum_{k=1}^N \left\langle\sum_{j=1}^N \mathbf{C}_{ik}p_{ik},\mathbf{v}_k\right\rangle$. If the cell in in the interior of Ω, then $\mathbf{C}_{ik}p_{ik} = 0$ by definition of the closure relation. If the cell is on the boundary, then $\mathbf{C}_{ik}p_{ik}$ is a vector parallel to the exterior normal, see (35-36). In both cases $\left\langle\sum_{j=1}^N \mathbf{C}_{ik}p_{ik},\mathbf{v}_k\right\rangle = 0$ for $1\le k\le N$ from which the claim is deduced. □

The consistency with the entropy inequality is obtained as a consequence of (28-29-30) combined with the closure relations (31-33) in the general case or (31-35-36) near the boundary.

Proposition 3.4. *Assume the Voronoï cell Ω_i shares no part with the boundary $\partial\Omega$. The scheme (28-29-30) combined with the closure relations (31-33) or (31-35-36) satisfy local entropy inequalities under the form*

$$\frac{d}{dt}S_i \ge 0 \text{ for all } 1\le i\le N.$$

Remark 3.5. *The satisfaction of the entropy inequality is beneficial for two reasons. The first reason is that it corresponds to the mathematical theory of weak solutions for hyperbolic equations. The second reason is that it is ultimately a way to guarantee to some non linear stability of the numerical method.*

Proof. The fundamental principle of thermodynamics yields the differential identity $TdS = d\varepsilon + pd\tau$ which is rewritten as $TdS = pd\tau - \langle\mathbf{u},d\mathbf{u}\rangle + de$ where the temperature is $T>0$ under normal conditions. So one has

$$M_iT_i\frac{d}{dt}S_i = p_iM_i\frac{d}{dt}\tau_i - \left\langle\mathbf{u}_i,M_i\frac{d}{dt}\mathbf{u}_i\right\rangle + \frac{d}{dt}e_i = p_i\sum_{k=1}^N\langle\mathbf{C}_{ik},\mathbf{v}_k\rangle + \left\langle\mathbf{u}_i,\sum_{k=1}^N\mathbf{C}_{ik}p_{ik}\right\rangle - \sum_{k=1}^N p_{ik}\langle\mathbf{C}_{ik},\mathbf{v}_k\rangle.$$

In the general case (31-33) the Voronoï cell Ω_i shares no part with the boundary $\partial\Omega$. In this case one has $\sum_{k=1}^N\mathbf{C}_{ik} = 0$ from which one gets

$$\sum_{k=1}^N p_i\langle\mathbf{C}_{ik},\mathbf{u}_i\rangle = 0. \tag{37}$$

Note that (37) also holds when the sliding condition is incorporated in the closure system, see (31-35-36). One obtains in both cases

$$M_iT_i\frac{d}{dt}S_i = p_i\sum_{k=1}^N\langle\mathbf{C}_{ik},\mathbf{v}_k\rangle + \left\langle\mathbf{u}_j,\sum_{k=1}^N\mathbf{C}_{ik}p_{ik}\right\rangle - \sum_{k=1}^N p_{ik}\langle\mathbf{C}_{ik},\mathbf{v}_k\rangle - \sum_{k=1}^N p_i\langle\mathbf{C}_{ik},\mathbf{u}_i\rangle$$

which can be factorized under the form $M_iT_i\frac{d}{dt}S_i = \sum_{k=1}^N(p_i-p_{ik})\langle\mathbf{C}_{ik},\mathbf{v}_k-\mathbf{u}_i\rangle$. Then (31) is common to the two cases. Therefore one gets $M_iT_i\frac{d}{dt}S_i = \sum_{k=1}^N\frac{\lambda_{ik}}{|\mathbf{C}_{ik}|}\langle\mathbf{C}_{ik},\mathbf{v}_k-\mathbf{u}_i\rangle^2 \ge 0$ which ends the proof. □

3.2 Fully discrete first-order scheme

We present the general scheme in any dimension $d\ge 2$, then we analyze the resulting method in the one dimensional case $d=1$.

3.2.1 The general form

The fully discrete first order scheme is obtained by using an explicit Euler discretization. The lagrangian masses M_i are initialized at initial time $t_0 = 0$. As it is usual, one uses (26) instead of (28) to predict the density. One obtains the following time loop where the discrete time is $t_n = n\Delta t$ and $\Delta t > 0$ is the time step.

• All generators $\mathbf{x}_k^n$ for $1 \leq k \leq N$ are known at the beginning of the time step. Then one generates the Voronoï cells and many subroutines are publicly available for this task. The volumes $|\Omega_i^n|$ are calculated for $1 \leq k \leq N$. The partial derivatives $\mathbf{C}_{ik}^n$ are calculated for $1 \leq i, k \leq N$.
• The values of the physical variables $\mathbf{u}_i^n$ and e_i^n are known from the previous time step. The density is recalculated using $\rho_i^n = M_i / |\Omega_i^n|$. Then the pressures p_i^n are calculated from the equation of state which is a perfect gas pressure law in our case.
• One solves the closure relations (31-33) or (31-35-36). It yields the discrete velocities $\mathbf{v}_k^n$ $1 \leq k \leq N$ and the pressures p_{ik}^n for all $1 \leq i, k \leq N$.
• One updates the velocity

$$M_i \frac{\mathbf{u}_i^{n+1} - \mathbf{u}_i^n}{\Delta t} = -\sum_{k=1}^{N} \mathbf{C}_{ik}^n \; p_{ik}^n, \qquad 1 \leq i \leq N, \tag{38}$$

and the total energy

$$M_i \frac{e_i^{n+1} - e_i^n}{\Delta t} = -\sum_{k=1}^{N} \langle \mathbf{C}_{ik}^n, \mathbf{v}_k^n \rangle \, p_{ik}^n, \qquad 1 \leq i \leq N. \tag{39}$$

• Finally one recalculates the new position of the generators

$$\mathbf{x}_k^{n+1} = \mathbf{x}_k^n + \Delta t \mathbf{v}_k^n, \qquad 1 \leq k \leq N. \tag{40}$$

This fully discrete directly inherits of the properties of the continuous-in-time scheme. It is conservative in local mass, conservative in total impulse up to the boundary and conservative in total energy. A CFL time step restriction is needed to reach numerical stability. The physical entropy increases under CFL as in [14, 7, 27, 26].

3.2.2 The scheme in 1D

It is instructing to write the scheme in dimension $d = 1$ because it will make evident two properties. The first property is that the scheme reduces to a special version of the Godunov lagrangian scheme. The second property is that the scheme is endowed with a odd-even decoupled structure.

We use the notations of Remark 2.7 and do not consider boundaries to simplify the analysis. With the notation (25), then the vectors (10) are scalars

$$C_{i,i\pm1} = \pm\frac{1}{2} \text{ and } C_{ik} = 0 \text{ for k } \neq \pm 1.$$

The discrete time evolution of the volume $V_i^n = \frac{1}{2}(x_{i+1}^n - x_{i-1}^n)$ is naturally

$$V_i^{n+1} = V_i^n + \frac{1}{2}\Delta t v_{i+1}^n - \frac{1}{2}\Delta t v_{i-1}^n.$$

Since the mass is preserved, one can rewrite this law as

$$M_i \frac{\tau_i^{n+1} - \tau_i^n}{\Delta t} = \frac{1}{2} v_{i+1}^n - \frac{1}{2} v_{i-1}^n. \tag{41}$$

The pressure closure identity (31) writes as

$$p_{i,i\pm1}^n - p_i^n \pm \rho_i^n c_i^n \left(v_{i\pm1}^n - u_i^n \right) = 0.$$

The equation for the velocity of the generators is

$$\frac{1}{2}(\rho_{i-1}^n c_{i-1}^n + \rho_{i+1}^n c_{i+1}^n) v_i^n = -\frac{1}{2}(p_{i+1}^n - \rho_{i+1}^n c_{i+1}^n u_{i+1}^n) + \frac{1}{2}(p_{i-1}^n + \rho_{i-1}^n c_{i-1}^n u_i^n)$$

which yields

$$v_i^n = \frac{\rho_{i-1}^n c_{i-1}^n u_i^n + \rho_{i+1}^n c_{i+1}^n u_{i+1}^n}{\rho_{i-1}^n c_{i-1}^n + \rho_{i+1}^n c_{i+1}^n} + \frac{p_{i-1}^n - p_{i+1}^n}{\rho_{i-1}^n c_{i-1}^n + \rho_{i+1}^n c_{i+1}^n}. \tag{42}$$

In dimension $d = 1$, the closure relation (33) imposes that the pressures are equal $p_{i-1,i} - p_{i+1,i} = 0$. It yields

$$p_{i-1,i} = p_{i+1,i} = \frac{\rho_{i+1}^n c_{i+1}^n p_i^n + \rho_{i-1}^n c_{i-1}^n p_{i+1}^n}{\rho_{i-1}^n c_{i-1}^n + \rho_{i+1}^n c_{i+1}^n} + \frac{\rho_{i-1}^n c_{i-1}^n \rho_{i+1}^n c_{i+1}^n}{\rho_{i-1}^n c_{i-1}^n + \rho_{i+1}^n c_{i+1}^n}(u_{i-1}^n - u_{i+1}^n). \tag{43}$$

One recognizes the formulas of the famous Godunov lagrangian scheme [21, 12]. The final scheme is closed by considering (38)

$$M_i \frac{u_i^{n+1} - u_i^n}{\Delta t} = -\frac{1}{2} p_{i,i+1}^n + \frac{1}{2} p_{i,i-1}^n \tag{44}$$

and (39)

$$M_i \frac{e_i^{n+1} - e_i^n}{\Delta t} = -\frac{1}{2} p_{i,i+1}^n v_{i+1}^n + \frac{1}{2} p_{i,i-1}^n v_{i-1}^n. \tag{45}$$

Since the mass is $M_i = \frac{1}{2}(x_{i+1}^n - x_{i-1}^n)\rho_i^n$, one can simplify the coefficient $\frac{1}{2}$ in all discrete equations (41), (44) or (45).

Lemma 3.6. *The one-dimensional scheme (41)-(44)-(45) with the solver (42)-(43) shows an odd-even decoupling.*

Proof. Consider $i = 2k$ which is even for simplicity. Then the discrete evolution equation (41) in cell $i = 2k$ shows that the discrete fluxes are calculated at $i + 1 = 2k + 1$ and $i - 1 = 2k - 1$. But the discrete fluxes (42) are themselves calculated in function of quantities evaluated at $i + 1 \pm 1$ and $i - 1 \pm 1$. Therefore the discrete evolution equation in cell $i = 2k$ is evaluated in function of quantities evaluated at $i - 2$ i and $i + 2$. The other equations (44) and (45) have the same structure. So finally the discrete evolution in the cell does not depend on closed neighbors $i - 1$ and $i + 1$, but on $i - 2 = 2k - 2$ and $i + 2 = 2k + 2$ which are even as well. This is the odd-even decoupling. □

Remark 3.7. *Due to this property, one expects some kind of numerical instability in discrete calculations. We will show this is indeed the case and it is the reason why a stabilizer is proposed in Section 4.2. The stabilizer reintroduces numerical interactions between closed neighbors. With the stabilizer, the 1D scheme cannot have the odd-even structure.*

4 Optimization of the numerical method

We describe two natural modifications or enhancements of the previous method.

4.1 Enhancement of 1D symmetries

Ley us assume that one starts from distribution of generators such that the ensemble of Voronoï cells is yields regular cartesian mesh, and that the flow is aligned with the initial mesh. It seems natural to evaluate if the scheme is able to preserve the cartesian structure at least in the direction of the flow. Basic tests show that the scheme with the closure (31-33) or (31-35-36) does not preserve the aligned-with-the-flow structure of the mesh even at the first iteration. Our goal hereafter is to show a simple modification which better preserves the cartesian structure.

With the notations of Section 2, we decompose the vector $\mathbf{C}_{ik}$ between a normal part $\mathbf{N}_{ik} = \sigma_{ik} \frac{\mathbf{n}_{ik}}{2}$ and a tangential part $\mathbf{T}_{ik} = -\sigma_{ik} \frac{\mathbf{x}^{jk} - \mathbf{x}_{jk}}{|\mathbf{x}_k - \mathbf{x}_i|}$

$$\mathbf{C}_{ik} = \mathbf{N}_{ik} + \mathbf{T}_{ik}.$$

Then (31) is decomposed as well between a normal part and a tangential part

$$\begin{cases} p_{ik}^{\mathbf{N}} - p_i + \mu_i^{\mathbf{N}} \lambda_{ik} \left\langle \mathbf{v}_k - \mathbf{u}_i, \frac{\mathbf{N}_{ik}}{|\mathbf{N}_{ik}|} \right\rangle = 0, \\ p_{ik}^{\mathbf{T}} - p_i + \mu_i^{\mathbf{T}} \lambda_{ik} \left\langle \mathbf{v}_k - \mathbf{u}_i, \frac{\mathbf{T}_{ik}}{|\mathbf{T}_{ik}|} \right\rangle = 0. \end{cases} \tag{46}$$

Remark 4.1. *One observes that the single acoustic Godunov relation (31) is now decoupled in two acoustic Godunov relations (46). This decoupling reflets the logic of the EUCCLHYD scheme with respect to the GLACE scheme, see [14, 7, 12, 27, 26].*

Here the new coefficients are $\mu_i^{\mathbf{N}} \geq 0$ and $\mu_i^{\mathbf{T}} \geq 0$. The identity (33) becomes

$$\sum_{i=1}^{N} \left(\mathbf{N}_{ik} p_{ik}^{\mathbf{N}} + \mathbf{T}_{ik} p_{ik}^{\mathbf{T}} \right) = 0.$$

Elimination of the pressures $p_{ik}^{\mathbf{N}}$ and $p_{ik}^{\mathbf{T}}$ yields the system

$$\left(\sum_{i=1}^{N} \mu_{ik}^{\mathrm{N}} \frac{\mathbf{N}_{ik} \otimes \mathbf{N}_{ik}}{|\mathbf{N}_{ik}|} + \mu_{ik}^{\mathrm{T}} \frac{\mathbf{T}_{ik} \otimes \mathbf{T}_{ik}}{|\mathbf{T}_{ik}|}\right) \mathbf{v}_k$$

$$= \sum_{i=1}^{N} \mathbf{N}_{ik} \left(p_i - \mu_{ik}^{\mathrm{N}} \left\langle \mathbf{u}_i, \frac{\mathbf{N}_{ik}}{|\mathbf{N}_{ik}|} \right\rangle\right) + \mathbf{T}_{ik} \left(p_i - \mu_{ik}^{\mathrm{T}} \left\langle \mathbf{u}_i, \frac{\mathbf{T}_{ik}}{|\mathbf{T}_{ik}|} \right\rangle\right) \quad \text{for all } k. \tag{47}$$

The calculation of the velocity $\mathbf{v}_k$ requires only the condition that the matrix in front of it is non singular. Instead of a complicated analysis, we postulate that the normal vectors $\mathbf{N}_{ik}$ are the classical ones in a finite volume scheme (multiplied by a factor $1/2$) and that the tangential vectors $\mathbf{T}_{ik}$ are the non standard ones which generate non standard numerical interactions. At the end of the analysis the non standard tangential vectors are the main cause of a potential loss of 1D symmetry (in the prediction of the velocity used for for the displacement of the generator). Having this principle in mind, a natural prescription is to diminish the influence of the tangential part as much as possible. A natural choice that fulfills this requirement is to take

$$\mu_{ik}^{\mathrm{N}} = 1 \text{ and } \mu_{ik}^{\mathrm{T}} = 0 \text{ for all } k. \tag{48}$$

Since $\mu_{ik}^{\mathrm{T}} = 0$ then no tangential vectors are taken into account, nor in the matrix and neither in the dissipative part of the fluxes in (47). Once the velocity is calculated, the pressures (46) are obtained and used to integrate the equations (38-39) with the vectors $\mathbf{N}_{ik}$ and $\mathbf{T}_{ik}$ instead of $\mathbf{C}_{ik}$. Note that all properties of the general scheme are preserved (conservation of mass, total impulse, total energy and increase of entropy). Some numerical test will be shown with this choice.

Remark 4.2. *It can be checked that this scheme reduces to the one dimensional scheme of Section 3.2.2.*

4.2 A stabilizer

The dynamics of a Voronoï mesh with moving generators can be singular if the some generators become too close. Moreover the extra-term $\frac{\mathbf{x}^{ik} - \mathbf{x}_{ik}}{|\mathbf{x}_k - \mathbf{x}_i|}$ in (10) is singular in the limit $|\mathbf{x}_k - \mathbf{x}_i| \to 0$. That is why a natural question is to introduce stabilizing terms (repulsive forces) in the solver when some generators become too close. We describe hereafter in dimension $d = 2$ a simple proposition which takes its origin in [11]. We rapidly show in the appendix why such stabilization is weakly consistent.

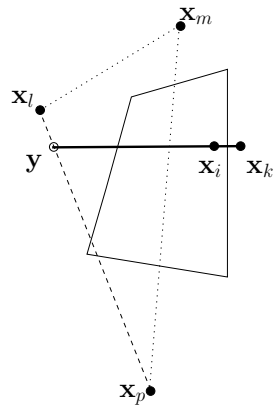

Figure 7: Alignement of the points $\mathbf{x}_j$, $\mathbf{x}_k$ and $\mathbf{y} = \alpha\mathbf{x}_p + \beta\mathbf{x}_l$. The fraction is $f_{ik} = \frac{|\mathbf{x}_i - \mathbf{x}_k|}{|\mathbf{y} - \mathbf{x}_k|}$.

The idea is to consider 4 generators, such as $\mathbf{x}_j$, $\mathbf{x}_k$, $\mathbf{x}_p$ and $\mathbf{x}_l$ as in Figure 7, in the case where two generators are sufficiently close that the situation is evaluated as a dangerous one. One sets

$$\mathbf{d} = \mathbf{x}_i - \mathbf{x}_k$$

and defines the point $\mathbf{y}$ which is at the intersection of the line $\{\mathbf{x}(t) = \mathbf{x}_j + t(\mathbf{x}_k - \mathbf{x}_j) \text{ for } t \in \mathbb{R}\}$ and of the line $\{\mathbf{y}(s) = \mathbf{x}_p + s(\mathbf{x}_l - \mathbf{x}_p) \text{ for } s \in \mathbb{R}\}$. We firstly find $0 \leq \alpha$ and $0 \leq \beta$ with $\alpha + \beta = 1$ such that

$$\alpha(\mathbf{x}_p - \mathbf{x}_i) + \beta(\mathbf{x}_l - \mathbf{x}_i) = \lambda(\mathbf{x}_i - \mathbf{x}_k) \quad \text{with } \lambda > 0. \tag{49}$$

Then we define the ratio of length $f_{ik} = \frac{|\mathbf{x}_i - \mathbf{x}_k|}{|\mathbf{y} - \mathbf{x}_k|}$.

We systematically select the pair $\mathbf{x}_p$ and $\mathbf{x}_l$ such that f_{ik} the smallest value among all possible pairs, as it is visible in the Figure 7. This ratio is evaluated via the function

$$\varphi^{ik}(\mathbf{x}_i, \mathbf{x}_k, \mathbf{x}_p, \mathbf{x}_l) = \frac{\langle \mathbf{x}_i - \mathbf{x}_k, \mathbf{d} \rangle}{\langle \alpha \mathbf{x}_p + \beta \mathbf{x}_l - \mathbf{x}_k, \mathbf{d} \rangle} \tag{50}$$

where the direction $\mathbf{d} = \frac{\mathbf{x}_i - \mathbf{x}_k}{|\mathbf{x}_i - \mathbf{x}_k|}$ is pre-calculated and the coefficients α and β are pre-calculated as well. Then the fraction

$$\varphi^{ik}(\mathbf{x}_i, \mathbf{x}_k, \mathbf{x}_p, \mathbf{x}_l)$$

will be our sensor to detect if $\mathbf{x}_i$ and $\mathbf{x}_k$ are becoming dangerously close. The reason why $\mathbf{d}$, α and β are written as frozen parameters will find a rigorous theoretical justification in the appendix.

One decides a certain small threshold $\varepsilon_* > 0$ and the idea is to activate the stabilization term when

$$\varphi^{ik}(\mathbf{x}_i, \mathbf{x}_k, \mathbf{x}_p, \mathbf{x}_l) < \varepsilon_*.$$

The way we use this function is to consider the potential

$$(\mathbf{x}_1, \dots, \mathbf{x}_N) \mapsto C \log \varphi^{ik}(\mathbf{x}_i, \mathbf{x}_k, \mathbf{x}_p, \mathbf{x}_l) \tag{51}$$

and to incorporate it in the total entropy for the cell Ω_j. Then the fundamental entropy law written in cell Ω_i is modified under the following form

$$M_i T_i \frac{d}{dt}(S_i + C \sum_k \log \varphi^{ik}) = M_i \frac{d}{dt} e_i - \left\langle \mathbf{u}_i, \frac{d}{dt} \mathbf{u}_i \right\rangle + p_i M_i \frac{d}{dt} \tau_i + \sum_k q^{ik} \sum_r \langle \mathbf{D}_r^{ik}, \mathbf{v}_r \rangle$$

where the last terms come from the chain rule, that is

$$q^{ik} = \frac{T_i C}{\varphi_{\mathbf{d},\alpha,\beta}(\mathbf{x}_i, \mathbf{x}_k, \mathbf{x}_p, \mathbf{x}_l))} \text{ and } \mathbf{D}_r^{ik} = \nabla_{\mathbf{x}_r} \varphi^{ik}_{\mathbf{d},\alpha,\beta}(\mathbf{x}_i, \mathbf{x}_k, \mathbf{x}_p, \mathbf{x}_l)).$$

Then q^{ik} is interpreted as a kind of new pressure and $\mathbf{D}_r^{ik}$ is interpreted as a kind of new direction vector like all the $\mathbf{C}_{ik}$. As a consequence of the definition of the potential (52), one has

$$\left\{ \begin{array}{rll} \mathbf{D}_r^{ik} = & \frac{1}{\langle \alpha \mathbf{x}_p + \beta \mathbf{x}_l - \mathbf{x}_k, \mathbf{d} \rangle} \mathbf{d} & \text{for } r = i, \\ \mathbf{D}_r^{ik} = & \left(\frac{\langle \mathbf{x}_i - \mathbf{x}_k, \mathbf{d} \rangle}{\langle \alpha \mathbf{x}_p + \beta \mathbf{x}_l - \mathbf{x}_k, \mathbf{d} \rangle^2} - \frac{1}{\langle \alpha \mathbf{x}_p + \beta \mathbf{x}_l - \mathbf{x}_k, \mathbf{d} \rangle} \right) \mathbf{d} & \text{for } r = k, \\ \mathbf{D}_r^{ik} = & -\alpha \frac{\langle \mathbf{x}_i - \mathbf{x}_k, \mathbf{d} \rangle}{\langle \alpha \mathbf{x}_p + \beta \mathbf{x}_l - \mathbf{x}_k, \mathbf{d} \rangle^2} \mathbf{d} & \text{for } r = p, \\ \mathbf{D}_r^{ik} = & -\beta \frac{\langle \mathbf{x}_i - \mathbf{x}_k, \mathbf{d} \rangle}{\langle \alpha \mathbf{x}_p + \beta \mathbf{x}_l - \mathbf{x}_k, \mathbf{d} \rangle^2} \mathbf{d} & \text{for } r = l, \\ \mathbf{D}_r^{ik} = & \mathbf{0} & \text{for } r \neq i, k, p, l. \end{array} \right. \tag{52}$$

As explained in [13], it is then easy to generalize the closure (31-33-34). The acoustic relation is (31) is generalized as

$$q_r^{ik} - q^{ik} + a_r^{ik} \left\langle \mathbf{v}_r - \mathbf{u}_i, \frac{\mathbf{D}_r^{ik}}{|\mathbf{D}_r^{ik}|} \right\rangle = 0, \quad \text{for all } i, k, r. \tag{53}$$

These new terms will be used in the update of the momentum equation (29) which becomes

$$M_i \frac{d}{dt} \mathbf{u}_i(t) = -\sum_{k=1}^N \mathbf{C}_{ik} p_{ik} - \sum_{k=1}^N \sum_{r=1}^N \mathbf{D}_r^{ik} q_r^{ik}.$$

The new terms are incorporated in the closure relation which becomes

$$\sum_{i=1}^N \mathbf{C}_{ik} p_{ik} - \sum_{i=1}^N \sum_{r=1}^N \mathbf{D}_r^{ik} q_r^{ik} = 0. \tag{54}$$

The coupled linear (31)-(53)-(54) is solved as follows. By elimination of the pressures p_{ik} and of the new terms q_r^{ik}, one firstly assembles the linear system

$$\left(\sum_{i=1}^N \lambda_{ik} \frac{\mathbf{C}_{ik} \otimes \mathbf{C}_{ik}}{|\mathbf{C}_{ik}|} + \sum_{i=1}^N \sum_{r=1}^N a_r^{ik} \frac{\mathbf{D}_{ik} \otimes \mathbf{D}_{ik}}{|\mathbf{D}_{ik}|} \right) \mathbf{v}_k$$

$$= \sum_{i=1}^N \mathbf{C}_{ik} \left(p_i - \lambda_{ik} \left\langle \mathbf{u}_i, \frac{\mathbf{C}_{ik}}{|\mathbf{C}_{ik}|} \right\rangle \right) + \sum_{i=1}^N \sum_{r=1}^N \mathbf{D}_r^{ik} \left(q^{ik} - a_r^{ik} \left\langle \mathbf{u}_i, \frac{\mathbf{D}_r^{ik}}{|\mathbf{D}_{ik}|} \right\rangle \right) \quad \text{for all } k.$$

The time-continuous energy equation (30) becomes

$$M_i \frac{d}{dt} e_i(t) = -\sum_{k=1}^{N} \langle \mathbf{C}_{ik}, \mathbf{v}_k \rangle \, p_{ik} - \sum_{k=1}^{N} \sum_{r=1}^{N} \left\langle \mathbf{D}_r^{ik}, \mathbf{v}_k \right\rangle q_r^{ik}.$$

This method can be adapted without any difficulty to the scheme of Section 4.1. Due to the equality (54) the method is conservative in total impulse up the the boundaries and in total energy. There is no term at the boundary for the energy because of the sliding boundary condition. It is easy to check that the entropy inequality takes now the form

$$M_i T_i \frac{d}{dt}(S_i + C \sum_k \log \varphi^{ik}) = \sum_{k=1}^{N} \frac{\lambda_{ik}}{|\mathbf{C}_{ik}|} \langle \mathbf{C}_{ik}, \mathbf{v}_k - \mathbf{u}_i \rangle^2 + \sum_{k=1}^{N} \sum_{r=1}^{N} \frac{a_r^{ik}}{|\mathbf{D}_r^{ik}|} \left\langle \mathbf{D}_r^{ik}, \mathbf{v}_k - \mathbf{u}_i \right\rangle^2 \geq 0.$$

The rationale behind the stabilizer is based on this generalized entropy inequality inequality. Since the constant is taken positive, that is $C > 0$, the numerical value of the fraction φ^{ik} cannot vanish, because it would imply a negative generalized entropy production. The specific form of potentials based on (50) is shown to be weakly consistant in the appendix.

5 Numerical illustrations

The numerical illustrations below were obtained with the general scheme constructed in this article. We complement the scheme with a CFL condition for the time step prediction. This CFL condition has been obtained by heuristic considerations which are standard for hyperbolic equations and lagrangian equations. Since the scheme is globally first order in space and time, we do not expect very accurate results. The sliding boundary condition is implemented with the mirror technique.

The scheme has been implemented in a basic research code written in Python with the library *Scipy-Voronoi* [31]. This library generates a Voronoï mesh in $\mathbb{R}^d$ from a set of generators. The time needed to generate the Voronoï mesh is in practice $O(N)$ (which is in accordance with the theoretical scaling $O(N \log N)$ [2]). It is necessary to post-process the result of the library in order to truncate the mesh in the finite domain $\Omega = [0, L_x] \times [0, L_y]$ and in order to calculate the vectors $\mathbf{C}_{jk}$.

Since the numerical method is lagrangian, it is well adapted to multi-fluid calculations. No complex multi-material ALE technique is needed to run such calculations and this is an important property in view of applications. For example all generators/Voronoï cells can embark their own value of the coefficient γ. It will be the case for some test problems below.

The potential function used in stabilizer is a slight modification of (51). It takes the form $C \log(\varphi - f_s)$ with $C = 0.05$ and $f_s = 0.1$ to guarantee some minimal distance between the generators.

5.1 Sod test problem

We plot the results obtained with the second variant for the one dimensional Sod shock tube test problem. We used 200×3 cells in the domain $[0, 1] \times [0, 0.01]$. A plot of the central part of the mesh at initial time is provided in Figure 8. At final time $T = 0.2$, the horizontal velocity, pressure, density and thermodynamical entropy are represented in Figure 9 after projection on a 3×60 grid for better visualization. One observes good accuracy with respect to the analytical solution [33], in particular with the numerical solution close to the analytical solution at contact discontinuity (CD), since $u^{\mathrm{CD}} = 0.927\ldots$ and $p^{\mathrm{CD}} = 0.303\ldots$.

A stabilization procedure, described in Section 4.2, has been used. This stabilization seems in this case just necessary to run the simulation until final time. The mesh at final time is plot in Figure 10. It is striking to observe that the mesh presents a strong deviation with respect to 1D symmetry, even if the rarefaction wave and the shock are clearly identified. What is also striking is that this mesh instability seems not to be an hindrance for the ability of the method to capture the correct physical profiles, as visible in Figure 9.

An interesting question is to identity the reason of the mesh instability. Is it the scheme by itself which presents some kind of instability? Is it the generation of the Voronoï cells with the chosen library (*Scipy-Voronoi* [31] in our case)? It is the coupling of the scheme with the library? Is it the stabilization procedure which reveals inadequate? We leave the examination of these issues for further research.

5.2 Sedov problem

We consider the numerical solution of the Sedov problem at time $t = 1$. The initial mesh and the final mesh are shown in Figure 11. The scatter plot of the density is reasonably accurate, in particular the expanding shock is at the correct location ($R = 1$ at $t = 1$) and the maximal density is close to the reference value $\rho^{\mathrm{ref}} = 6$.

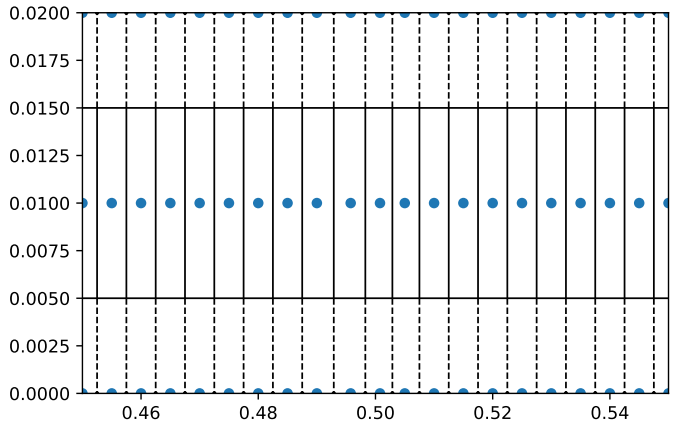

Figure 8: Zoom on the mesh structure at time $t = 0$ (horizontal axis is x, vertical axis is y). The dashed lines indicate that the Voronoï cells have an extension to infinity, which is truncated in finite domain Ω. The generators are indicated with the bullets.

5.3 A bi-fluid Sod problem in 2D

Here we consider a bi-fluid divergent Sod shock problem between two states separated by an interface at radius $R = 0.5$. The initial data are $p = \rho = 1$, $\mathbf{u} = 0$ and $\gamma_{\text{int}} = 3$ for $x^2 + y^2 < R^2$, and $p = 0.1$, $\rho = 0.125$, $\mathbf{u} = 0$ and $\gamma_{\text{ext}} = 1.4$ for $x^2 + y^2 > R^2$. The initial mesh is cartesian, not because it is adapted to the physics of this problem (it is not), but because the dynamical reconnection process of moving Voronoï meshes if more visible on the final plot of the mesh at time $T = 0.2$ (se Figure 13).

On this problem, no mesh instability similar to the Figure 10 has ever been observed. In particular the natural $x \leftrightarrow y$ symmetry with respect to reflexion at 45 degrees seem satisfied even by the final mesh.

5.4 Air-R22 shock/cylinder interaction test

This problem is representative of shock through Air on a bubble of R22 gas. It comes from a long series of numerical modeling works initiated in [29]. We take the data from [23]. The initial mesh is a R22 bubble in a domain $[0, 0.49] \times [0, 0.089]$ filled with air. A shock initially at $x = 0.275$ propagates through the left and hits the R22 bubble (radius 0.025, center at $(0.225, 0.445)$). The initial data are given in Table 1. The mesh at initial time and at final time $t = (60 + 540)10^{-6}$ are represented in Figure 14. The total number of generators $N = 3796$ is much lower than the total number of cells used in the simulations reported in [23] which is equal to 5000×1000. The numerical method is only first order so we do not expect very accurate results. Despite this fact, the global dynamics of the bubble seems in global accordance with the result [23, Fig. 19 t=540ms]. We also plot in Figure 15 the velocity field at final time obtained with our scheme. A vortical velocity is captured, in accordance with the later development of the bubble [23, Fig. 19 t=540ms].

Location	Density	Pressure	$\mathbf{u}$	γ
Air (post-shock)	1.686	1.5×10^5	(-113.5,0)	1.4
Air (pre-shock)	1.225	1.01325×10^5	(0,0)	1.4
R22	3.863	1.01325×10^5	(0,0)	1.249

Table 1: Initial values for the Air-R22 shock interaction

5.5 A three-fluid Greshko vortex

Finally we consider a Greshko vortex with the data from [32]. This problem has no shock so is slightly outside the scope of this work. The only difference with respect to [32] is that we use three different values of γ

$$\gamma = 2 \text{ for } R < 0.2, \quad \gamma = 1.4 \text{ for } 0.2 < R < 0.4 \text{ and } \gamma = 3 \text{ for } 0.4 < R$$

where the radius is $R = \sqrt{(x - L_x/2)^2 + (y - L_y)^2}$. The vorticity is such that interior part of the vortex turns of one quarter at the final time $t = \pi/10$. The initial ($t = 0$) and final ($t = \pi/10$) meshes are plotted in Figure 16. The fact that the scheme is only first order is a limitation in terms of accuracy of the results, however the interior part of the vortex points in the correct direction as shown by the markers.

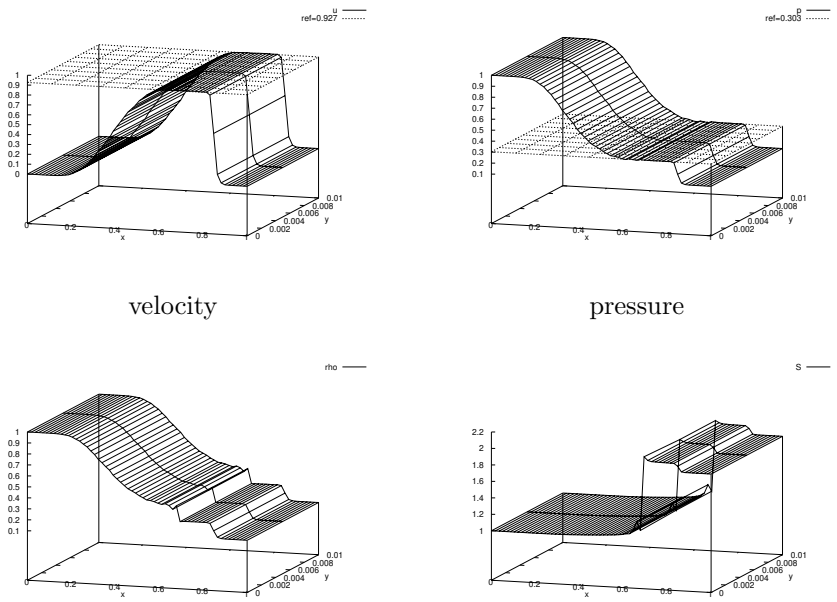

velocity pressure

density thermodynamical entropy

Figure 9: Final velocity, pressure, density and thermodynamical entropy for the Sod shock test problem.

A Weak consistency of the gradient operator

Consistency is not an evident property for particle methods [34]. A partial consistency analysis for linear profiles interpolated at centroids or generators is in [32]. On the other hand it is known that cell centered lagrangian fluid solvers are weakly consistant with the Euler system (23), see [12, page 290]. Here we extend the most essential part of the weak consistency analysis for the discrete pressure operator. We do not stick to absolute rigor but prefer to explain the main idea. For simplicity we take $\Omega = \mathbb{R}^d$.

Let us assume that a pressure function $\mathbf{x} \mapsto p(\mathbf{x})$ and a velocity function $\mathbf{x} \mapsto \mathbf{u}(\mathbf{x})$ are smooth functions. Sampling the pressure at the generators yields the pressure values $p_i = p(\mathbf{x}_i)$ for all i. Similarly sampling the velocity field at the generators yields the velocity values $\mathbf{u}_i = \mathbf{u}(\mathbf{x}_i)$ for all i. Then we consider the pressures p_{ik} constructed by (31)-(34). It yields the discrete pressure gradient

$$(\nabla p)_h(\mathbf{x}) = \frac{1}{V_i} \sum_k \mathbf{C}_{ik} p_{ik}. \tag{55}$$

Here $h > 0$ refers to the mean mesh size, and the mesh is assumed to be regular (that is all Voronoï cells are assumed to be non degenerate and of size comparable to h). The regime $h \to 0$ means that the space is filled by an arbitrarily large number of cells. We will make use of the a priori scalings $V_i = O(h^d)$ and $\mathbf{C}_{ik} = O(h^{d-1})$.

Following [12], we say that the discrete pressure gradient is weakly consistant if

$$\lim_{h \to 0} \int_{\mathbb{R}^d} (\nabla p)_h(\mathbf{x}) \varphi(\mathbf{x}) dx = - \int_{\mathbb{R}^d} p(\mathbf{x}) \ \nabla \varphi(\mathbf{x}) dx \tag{56}$$

for all smooth test function φ with compact support, where one can take $\varphi \in C_0^\infty(\mathbb{R}^d)$. The analysis is as follows. One writes

$$\int_{\mathbb{R}^d} (\nabla p)_h(\mathbf{x}) \varphi(\mathbf{x}) dx = \sum_i \frac{1}{V_i} \sum_k \mathbf{C}_{ik} p_{ik} \int_{\Omega_i} \varphi(\mathbf{x}) dx = \sum_i \frac{1}{V_i} \sum_k \mathbf{C}_{ik} p_{ik} V_i (\varphi(\mathbf{x}_i) + O(h))$$

$$= \left(\sum_i \frac{1}{V_i} \sum_k \mathbf{C}_{ik} p_{ik} V_i \varphi(\mathbf{x}_i) \right) + O(h) = \sum_k \left(\sum_i \mathbf{C}_{ik} p_{ik} \varphi(\mathbf{x}_i) \right) + O(h).$$

Using the equality of forces (31), one has also

$$\int_{\mathbb{R}^d} (\nabla p)_h(\mathbf{x}) \varphi(\mathbf{x}) dx = \sum_k \left(\sum_i \mathbf{C}_{ik} p_{ik} (\varphi(\mathbf{x}_i) - \varphi(\mathbf{x}_k)) \right) + O(h).$$

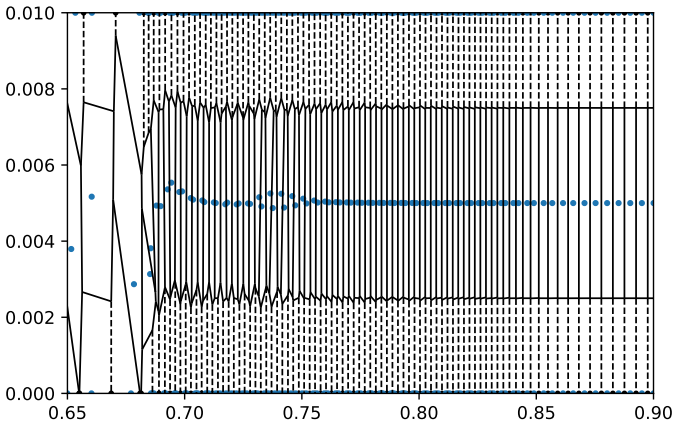

Figure 10: Zoom on the mesh structure at final time (horizontal axis is x, vertical axis is y). The mesh presents a strong deviation with respect to perfect 1D symmetry.

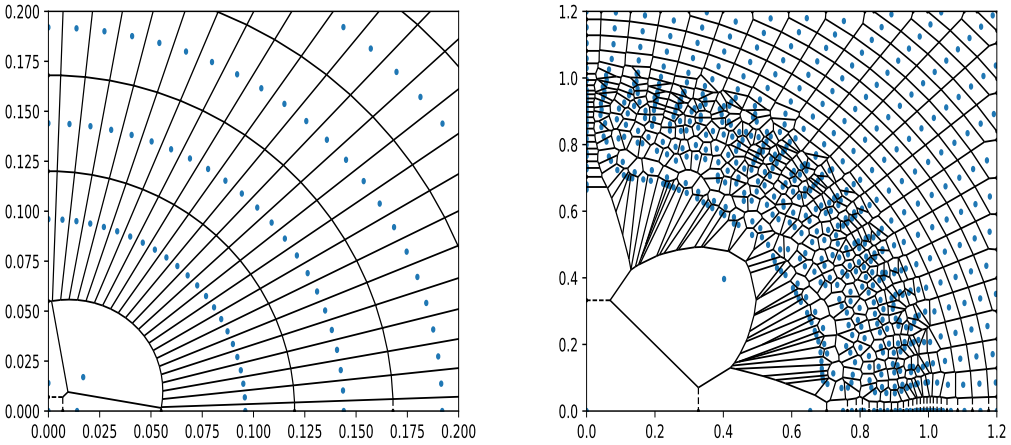

Figure 11: Initial mesh and final mesh for the Sedov problem.

One has the Taylor approximation $\varphi(\mathbf{x}_i) - \varphi(\mathbf{x}_k) = (\mathbf{x}_i - \mathbf{x}_k) \cdot \nabla\varphi(\mathbf{x}_i) + O(h^2)$. Under standard conditions [12], one has $p_{ik} = p(\mathbf{x}_i) + O(h)$. So one can write

$$\int_{\mathbb{R}^d} (\nabla p)_h(\mathbf{x})\varphi(\mathbf{x})dx = \sum_k \left(\sum_i \mathbf{C}_{ik} p(\mathbf{x}_i)(\mathbf{x}_i - \mathbf{x}_k) \cdot \nabla\varphi(\mathbf{x}_i) \right) + O(h)$$

$$= \sum_i p(\mathbf{x}_i) \left(\sum_k \mathbf{C}_{ik} \otimes (\mathbf{x}_i - \mathbf{x}_k) \right) \nabla\varphi(\mathbf{x}_i) + O(h).$$

We will make use of the following result.

Lemma A.1. *One has* $\sum_k \mathbf{C}_{ik} \otimes (\mathbf{x}_i - \mathbf{x}_k) = -V_i I_d + \sum_k A_{ik}$ *where* $A_{ik} = A_{ik}^t = -A_{ki}$.

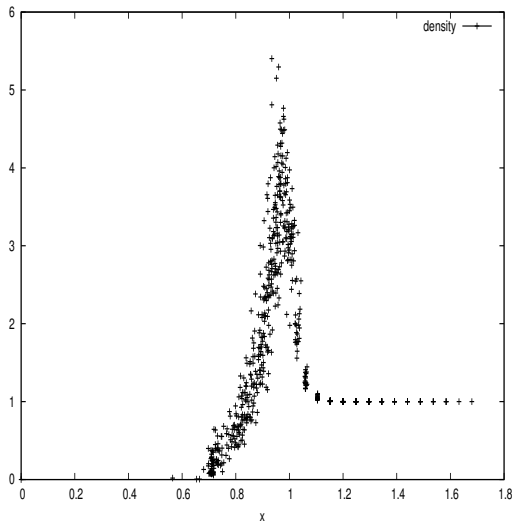

Figure 12: Density at final time for the Sedov problem.

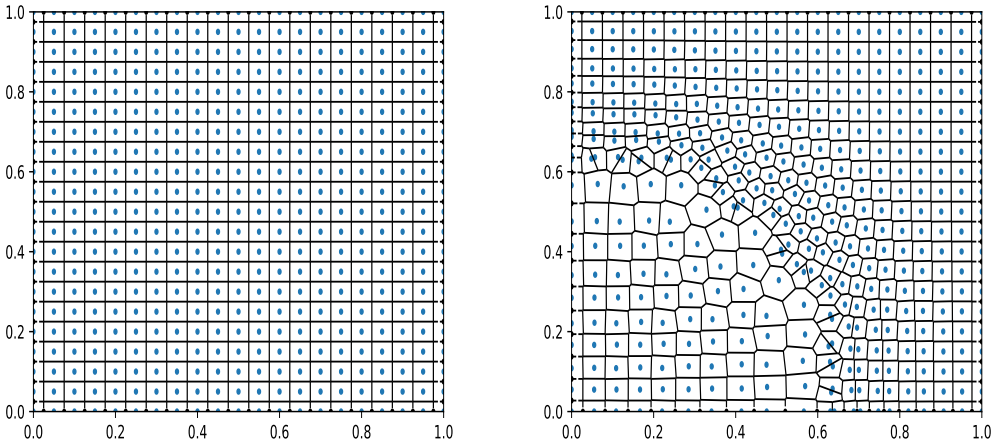

Figure 13: Sod problem calculated on a cartesian mesh.

Proof. One eliminates the vectors $\mathbf{C}_{ik}$ with (10). It yields

$$\begin{aligned}
\sum_k \mathbf{C}_{ik} \otimes (\mathbf{x}_i - \mathbf{x}_k) = & \quad \frac{1}{2}\sum_k \sigma_{ik}\ \mathbf{n}_{ik} \otimes (\mathbf{x}_i - \mathbf{x}_k) - \sum_k \frac{\sigma_{ik}}{|\mathbf{x}_i - \mathbf{x}_k|}(\mathbf{x}^{ik} - \mathbf{x}_{ik}) \otimes (\mathbf{x}_i - \mathbf{x}_k) \\
= & \quad -\frac{1}{2}\sum_k \sigma_{ik}\ \mathbf{n}_{ik} \otimes (\mathbf{x}_i + \mathbf{x}_k) - \sum_k \frac{\sigma_{ik}}{|\mathbf{x}_i - \mathbf{x}_k|}(\mathbf{x}^{ik} - \mathbf{x}_{ik}) \otimes (\mathbf{x}_i - \mathbf{x}_k) \\
= & \quad -\sum_k \sigma_{ik}\ \mathbf{n}_{ik} \otimes \mathbf{x}_{ik} - \sum_k \frac{\sigma_{ik}}{|\mathbf{x}_i - \mathbf{x}_k|}(\mathbf{x}^{ik} - \mathbf{x}_{ik}) \otimes (\mathbf{x}_i - \mathbf{x}_k) \\
= & -\sum_k \sigma_{ik}\ \mathbf{n}_{ik} \otimes \mathbf{x}^{ik} + \sum_k \sigma_{ik}\ \mathbf{n}_{ik} \otimes (\mathbf{x}^{ik} - \mathbf{x}_{ik}) - \sum_k \frac{\sigma_{ik}}{|\mathbf{x}_i - \mathbf{x}_k|}(\mathbf{x}^{ik} - \mathbf{x}_{ik}) \otimes (\mathbf{x}_i - \mathbf{x}_k) \\
= & \quad -V_i I_d + \sum_k \sigma_{ik}\ \mathbf{n}_{ik} \otimes (\mathbf{x}^{ik} - \mathbf{x}_{ik}) - \sum_k \frac{\sigma_{ik}}{|\mathbf{x}_i - \mathbf{x}_k|}(\mathbf{x}^{ik} - \mathbf{x}_{ik}) \otimes (\mathbf{x}_i - \mathbf{x}_k) \\
= & \quad -V_i I_d + \sum_k A_{ik}
\end{aligned}$$

where $A_{ik} = \frac{\sigma_{ik}}{|\mathbf{x}_i - \mathbf{x}_k|}\ (\mathbf{x}_i - \mathbf{x}_k) \otimes (\mathbf{x}^{ik} - \mathbf{x}_{ik}) - \frac{\sigma_{ik}}{|\mathbf{x}_i - \mathbf{x}_k|}(\mathbf{x}^{ik} - \mathbf{x}_{ik}) \otimes (\mathbf{x}_i - \mathbf{x}_k)$. By construction the matrix A_{ik} is anti-symmetric. Since $\mathbf{x}^{ik} - \mathbf{x}_{ik} = \mathbf{x}^{ki} - \mathbf{x}_{ki}$, then $A_{ik} = -A_{ki}$. □

Under standard conditions such that $\frac{\sigma_{ik}}{|\mathbf{x}_i - \mathbf{x}_k|} = O(1)$ is uniformly bounded with respect to h, one can continue

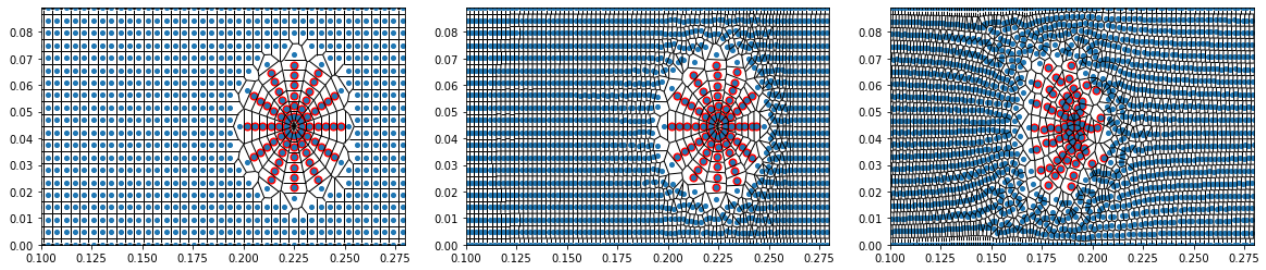

Figure 14: Initial mesh, intermediate and final mesh for the Air-R22 shock/cylinder interaction test. The numerical shock wave is visible on the right of the central plot at intermediate time.

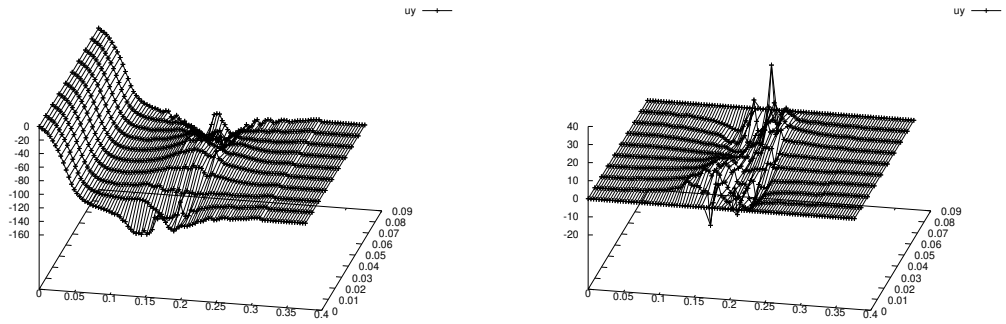

Figure 15: Velocity field u_x and u_y at final time for the Air-R22 shock/cylinder interaction test.

the previous analysis. It yields

$$\int_{\mathbb{R}^d} (\nabla p)_h(\mathbf{x})\varphi(\mathbf{x})dx = -\sum_i p(\mathbf{x}_i)\nabla\varphi(\mathbf{x}_i)V_i + \sum_i p(\mathbf{x}_i)(\sum_k A_{ik})\nabla\varphi(\mathbf{x}_i) + O(h).$$

$$\sum_i p(\mathbf{x}_i)\nabla\varphi(\mathbf{x}_i)V_i + \sum_i \sum_{k<i} A_{ik}(p(\mathbf{x}_i)\nabla\varphi(\mathbf{x}_i) - p(\mathbf{x}_k)\varphi(\mathbf{x}_k)) + O(h).$$

Since $|p(\mathbf{x}_i)\nabla\varphi(\mathbf{x}_i) - p(\mathbf{x}_k)\varphi(\mathbf{x}_k)| = O(h)$, φ is with compact support and $|A_{ik}| = O(h^2)$, one obtains

$$\int_{\mathbb{R}^d} (\nabla p)_h(\mathbf{x})\varphi(\mathbf{x})dx = -\sum_i p(\mathbf{x}_i)\nabla\varphi(\mathbf{x}_i)V_i + O(h) = -\int_{\mathbb{R}^d} p(\mathbf{x})\nabla\varphi(\mathbf{x})dx + O(h).$$

This formula is the weak consistency property (56).

Finally we indicate the main reason why the stabilizer of Section 4.2 preserves the formal weak consistency of the gradient operator which is now

$$(\nabla p)_h(\mathbf{x}) = \frac{1}{V_i}\left(\sum_k \mathbf{C}_{ik}p_{ik} + \sum_k \sum_r \mathbf{D}_r^{ik} q_r^{ik}\right). \tag{57}$$

To obtain the property of weak consistency, it is sufficient to reproduce the previous arguments until one uses the following lemma which is the counterpart of Lemma A.1.

Lemma A.2. *One has the identity* $\sum_r \mathbf{D}_r^{ik} \otimes (\mathbf{x}_i - \mathbf{x}_r) = 0$.

Proof. The vectors (52) are such that $\sum_r \mathbf{D}_r^{ik} = 0$ since $\alpha + \beta = 1$. Let us set

$$\mu = \langle \alpha\mathbf{x}_p + \beta\mathbf{x}_l - \mathbf{x}_k, \mathbf{d}\rangle \text{ and } \tau = \langle \mathbf{x}_i - \mathbf{x}_k, \mathbf{d}\rangle.$$

One can check that

$$\sum_r \mathbf{D}_r^{ik} \otimes \mathbf{x}_r = \mathbf{d} \otimes \left(\frac{1}{\mu}\mathbf{x}_i + \left(\frac{\tau}{\mu^2} - \frac{1}{\mu}\right)\mathbf{x}_k - \alpha\left(\frac{\tau}{\mu^2}\right)\mathbf{x}_p - \beta\left(\frac{\tau}{\mu^2}\right)\mathbf{x}_l\right)$$

$$= \frac{\tau}{\mu}\mathbf{d} \otimes \left(\frac{1}{\tau}(\mathbf{x}_i - \mathbf{x}_k) + \frac{1}{\mu}(\mathbf{x}_k - \alpha\mathbf{x}_p - \beta\mathbf{x}_l)\right)$$

The alignement constraint (49) yields that the vectors are aligned. So the whole quantity vanishes. □

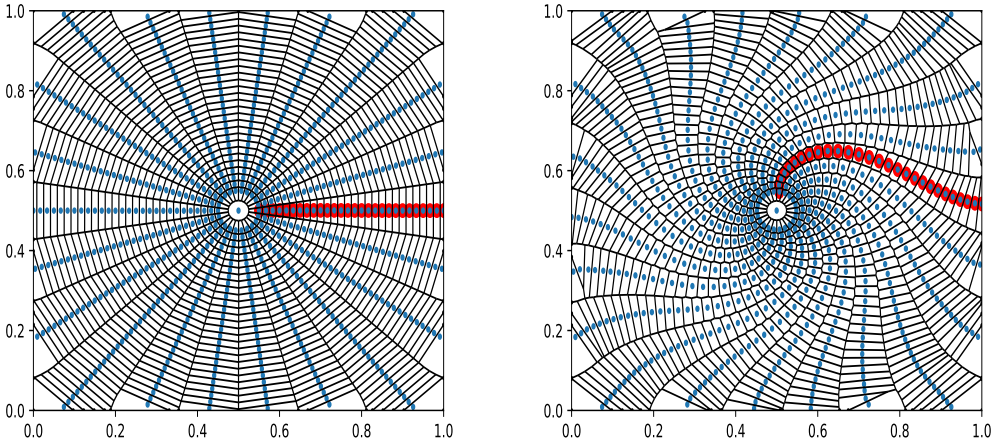

Figure 16: Initial mesh and final mesh for the three-fluid Greshko vortex. The markers line tangent to the vertical line is in accordance with the exact solution.

B A geometrical proof of the closed form formula in a simple case

We show below a simple geometrical proof of the closed form formula in dimension $d = 2$ in the situation depicted in Figure 17. We consider the five generators $\mathbf{x}_i = (\alpha\Delta x, \beta\Delta x)$, $\mathbf{x}_k = (\alpha\Delta x, (2-\beta)\Delta x)$, $\mathbf{x}_l = (-\alpha\Delta x, \beta\Delta x)$, $\mathbf{x}_m = (\alpha\Delta x, -\beta\Delta x)$ and $\mathbf{x}_n = ((2-\alpha)\Delta x, \beta\Delta x)$ where the parameters are $0 < \alpha, \beta < 1$ and $\Delta x > 0$. The cell Ω_i is a square with vertices $\mathbf{0} = (0,0)$, $\mathbf{A} = (0, \Delta x)$, $\mathbf{B} = (\Delta x, \Delta x)$ and $\mathbf{C} = (\Delta x, 0)$. The initial volume is $|\Omega_i| = \Delta x^2$.

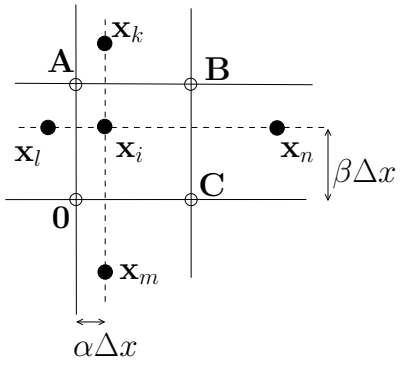

Figure 17: A square Voronoï cell with non equidistant generators.

Consider that all generators are fixed except $\mathbf{x}_k$ which moves to new position $\overline{\mathbf{x}_k} = (\mu, \nu)$ as shown in Figure 18. The equation of the equidistant line between $\mathbf{x}_i$ and $\overline{\mathbf{x}_k}$ is
$\mathcal{D} = \left\{(x,y) \mid \left(x - \frac{1}{2}(\mu + \alpha\Delta x)\right)(\mu - \alpha\Delta x) + \left(y - \frac{1}{2}(\nu + \beta\Delta x)\right)(\nu - \beta\Delta x) = 0\right\}$ that is

$$x(\mu - \alpha\Delta x) + y(\nu - \beta\Delta x) = \frac{1}{2}\left(\mu^2 + \nu^2 - (\alpha^2 + \beta^2)\Delta x^2\right). \tag{58}$$

The vertex $\mathbf{A}$ has moved as well to new position $\overline{\mathbf{A}} = (x_1, y_1) \in \mathcal{D} \cap \{x = 0\}$. Since $x_1 = 0$ one can calculate y_1 with (58) so

$$\overline{\mathbf{A}} = \left(0, \frac{\mu^2 + \nu^2 - (\alpha^2 + \beta^2)\Delta x^2}{2(\nu - \beta\Delta x)}\right).$$

The vertex $\mathbf{B}$ has moved as well to new position $\overline{\mathbf{B}} = (x_2, y_2) \in \mathcal{D} \cap \{x = \Delta x\}$. So $x_2 = \Delta x$ and one obtains

$$\overline{\mathbf{B}} = \left(\Delta x, \frac{\mu^2 + \nu^2 - (\alpha^2 + \beta^2)\Delta x^2 - 2\Delta x(\mu - \alpha\Delta x)}{2(\nu - \beta\Delta x)}\right).$$

The trapezoidal rule yields $\overline{|\Omega_i|} = \Delta x \times \frac{y_1 + y_2}{2} = \Delta x \times \frac{\mu^2 + \nu^2 - (\alpha^2 + \beta^2)\Delta x^2 - \Delta x(\mu - \alpha\Delta x)}{2(\nu - \beta\Delta x)}$. Now one calculate the partial derivatives $\partial_\mu \overline{|\Omega_i|} = \Delta x \times \frac{2\mu - \Delta x}{2(\nu - \beta\Delta x)}$ and $\partial_\nu \overline{|\Omega_i|} = \Delta x \times \frac{2\nu}{2(\nu - \beta\Delta x)} - \Delta x \times \frac{\mu^2 + \nu^2 - (\alpha^2 + \beta^2)\Delta x^2 - \Delta x(\mu - \alpha\Delta x)}{2(\nu - \beta\Delta x)^2}$.

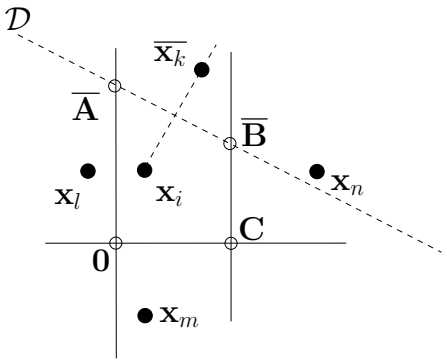

Figure 18: Evolution of the Voronoï cell.

The evaluation of the partial derivatives at the initial position is obtained by taking $\mu = \alpha\Delta x$ and $\nu = (2-\beta)\Delta x$. One gets

$$\partial_\mu \overline{|\Omega_i|}(\mathbf{x}_k) = \Delta x \times \frac{\alpha\Delta x - \Delta x/2}{(2-2\beta)\Delta x} \tag{59}$$

and

$$\partial_\nu \overline{|\Omega_i|}(\mathbf{x}_k) = \Delta x \times \frac{(2-\beta)\Delta x}{(2-2\beta)\Delta x} - \Delta x \times \frac{(2-\beta)^2\Delta x^2 - \beta^2\Delta x^2}{2(2-2\beta)^2\Delta x)^2}$$

$$= \Delta x \times \left(\frac{(2-\beta)}{2(1-\beta)} - \frac{4(1-\beta)}{8(1-\beta)^2}\right) = \Delta x \times \left(\frac{2-\beta}{2(1-\beta)} - \frac{1}{2(1-\beta)}\right) = \frac{\Delta x}{2}. \tag{60}$$

These results (59-60) are easy to interpret geometrically on Figure 17. One recognizes the tangential (60) contribution and the normal (59) contribution that show up in the general result (10).

References

[1] F.L. Addessio, J.R. Baumgardner, J.K. Dukowicz, N.L. Johnson, B.A. Kashiwa, R.M. Rauenzahn and C. Zemach, CAVEAT: A computer code for fluid dynamics problems with large distortion and internal slip, Technical Report, `https://www.osti.gov/biblio/10143914`, 1992.

[2] J.D. Boissonat and M. Yvinec, Algorithmic Geometry. Cambridge University Press, 1998.

[3] D. Boltcheva and B. Lévy, Surface reconstruction by computing restricted Voronoi cells in parallel, Computer-Aided Design, Volume 90, 2017.

[4] M. Campos Pinto, S. Jund, S. Salmon and E. Sonnendrücker, Charge-conserving FEMPIC schemes on general grids, Comptes Rendus Mécanique, Volume 342, Pages 570-582, 2014.

[5] M. Campos Pinto and F. Charles, Uniform Convergence of a Linearly Transformed Particle Method for the Vlasov–Poisson System, SIAM Journal on Numerical AnalysisVol. 54, Iss. 1, 2016.

[6] E.J. Caramana, D.E. Burton, M.J. Shashkov and P.P. Whalen, The Construction of Compatible Hydrodynamics Algorithms Utilizing Conservation of Total Energy, Journal of Computational Physics, Volume 146, Issue 1, Pages 227-262, 1998.

[7] G. Carré, S. Del Pino, B. Després and E. Labourasse A cell-centered lagrangian hydrodynamics scheme on general unstructured meshes in arbitrary dimension J. Comput. Phys., 228, pp. 5160-5183, 2009.

[8] G.H. Cottet, Multi-physics and particle methods. In Computational Fluid and Solid Mechanics, 1296-1298. Elsevier Science Ltd. 2003.

[9] C. Dafermos, Hyperbolic Conservation Laws in Continuum Physics, Springer, Grundlehren der mathematisch, 2016.

[10] S. Del Pino and I. Marmajou, Triangular metric-based mesh adaptation for compressible multi-material flows in semi-lagrangian coordinates, Journal of Computational Physics, Volume 478, 2023.

[11] B. Després, Weak consistency of the cell-centered lagrangian GLACE scheme on general meshes in any dimension, Computer Methods in Applied Mechanics and Engineering, Volume 199, Issues 41-44, Pages 2669-2679, 2010.

[12] B. Després, Numerical methods for Eulerian and lagrangian conservation laws. Birkhäuser, 2017.

[13] B. Després and E. Labourasse, Stabilization of cell-centered compressible lagrangian methods using subzonal entropy, Journal of Computational Physics, Volume 231, Issue 20, 2012,

[14] B. Després and C. Mazeran lagrangian gas dynamics in 2D and lagrangian systems Arch. Ration. Mech. Anal., 178 (2005), pp. 327-372.

[15] O. Devillers, M. Golin, K. Kedem and S. Schirra, Queries on Voronoi diagrams of moving points, Computational Geometry, Volume 6, Issue 5, 1996, Pages 315-327.

[16] D. Duque, A unified derivation of Voronoi, power, and finite-element lagrangian computational fluid dynamics, European Journal of Mechanics - B/Fluids, Volume 98, Pages 268-278, 2023.

[17] E.G. Flekkoy and P.V. Coveney, From molecular dynamics to dissipative particle dynamics Physical Review Letters 83 (9), 1775, 1999.

[18] E. Gaburro, W. Boscheri, S. Chiocchetti, C. Klingenberg, V. Springel and M. Dumbser, High order direct Arbitrary-Lagrangian-Eulerian schemes on moving Voronoi meshes with topology changes, Journal of Computational Physics, Volume 407, 2020.

[19] G. Guibas, L. Mitchell and J. Thomasroos, Voronoi Diagrams of Moving Points. International Journal of Computational Geometry and Applications, 2011.

[20] E. Godlewski and P.-A. Raviart, Numerical Approximation of Hyperbolic Systems of Conservation Laws, Springer New York, NY, 1996.

[21] S. K. Godunov, A. V. Zabrodin, M. Ya. Ivanov, A. N. Kraiko and G. P. Prokopov, Numerical Solving Many-Dimensional Problems of Gas Dynamics, Nauka, 1976.

[22] F. Hermeline, Triangulation automatique d'un polyèdre en dimension N. RAIRO. Analyse numérique, Tome 16 (1982) no. 3, pp. 211-242. `http://www.numdam.org/item/M2AN_1982__16_3_211_0/`

[23] S. Kokh and F. Lagoutière, An Anti-Diffusive Numerical Scheme for the Simulation of Interfaces between Compressible Fluids by Means of a Five-Equation Model, Journal of computational physics, 229, 2273-2809, 2010.

[24] B. Lévy and Y. Liu, L_p centroidal Voronoi Tesellation and applications, ACM transations in graphics, Volume 29, 2010.

[25] R. Loubere, P.H. Maire, M. Shashkov, J. Breil and S. Galera, ReALE: a reconnection-based arbitrary-Lagrangian-Eulerian method Journal of Computational Physics 229 (12), 4724-4761, 2010.

[26] P.H. Maire, R. Abgrall, J. Breil and J. Ovadia A cell-centered lagrangian scheme for 2D compressible flow problems SIAM J. Sci. Comput., 29, 2007.

[27] P.H. Maire, A high-order cell centered lagrangian scheme for two-dimensional compressible fluid flows on unstructured meshes J. Comput. Phys., 228 (7), pp. 2391-2425, 2009.

[28] J.J. Monaghan, An introduction to SPH, Computer Physics Communications, Volume 48, Issue 1, Pages 89-96, 1988.

[29] J.J. Quirk and S. Karni, On the Dynamics of a Shock Bubble Interaction. Journal of Fluid Mechanics, 318, 1291-163, 1996.

[30] M. Serrano and P. Espanol, Thermodynamically consistent mesoscopic fluid particle model, Physical Review E, Vol 64, 046115, 2000.

[31] Scipy-Voronoi, `https://docs.scipy.org/doc/scipy/reference/generated/scipy.spatial.Voronoi.html`

[32] V. Springel, E pur si muove: Galiliean-invariant cosmological hydrodynamical simulations on a moving mesh, Mon. Not. R. Astron. Soc., 2009.

[33] E. Toro, Riemann Solvers and Numerical Methods for Fluid Dynamics - A Practical Introduction, Springer, 1999.

[34] J. P. Vila, On particle weighted methods and smooth particle hydrodynamics, Mathematical models and methods in applied sciences, 9, 02, 161-209, 1999.

[35] J. von Neumann and R.D. Richtmyer, A method for the calculation of hydrodynamics shocks J. Appl. Phys., 21, pp. 232-237, 1950.